

University of Verona  
Department of Biotechnology

DOCTORAL PROGRAM IN  
Nanotechnologies and Nanostructured Materials for Biomedical  
Applications

with the financial contribution of  
EU funded FP7 ALPINE project, n. 229231

# **New Fabrication Approaches for High Efficiency CdS/CdTe Solar Cells**

Cycle XXV, 2010

S.S.D. FIS 01

Coordinator: Prof. Adolfo Speghini

Tutor: Dr. Alessandro Romeo

Doctoral Student: **M.Sc. Andrei Salavei**



*Deo Juvante*



# Contents

<b>Summary</b> .....	<b>1</b>
<b>1 Introduction</b> .....	<b>3</b>
1.1 Thin film CdS/CdTe solar cells.....	3
1.2 Historical overview of CdTe photovoltaic .....	7
1.3 Current research directions .....	9
1.4 References .....	11
<b>2 Aim of this work</b> .....	<b>17</b>
<b>3 The CdS/CdTe solar cell. Fabrication process and characterization</b> .....	<b>19</b>
3.1 Introduction.....	19
3.2 Substrate.....	19
3.3 Front contact .....	20
3.4 CdS deposition .....	21
3.5 CdTe deposition .....	22
3.6 CdCl <sub>2</sub> treatment.....	22
3.7 Back contact formation .....	23
3.8 Current-voltage measurements.....	24
3.9 Atomic Force Microscopy .....	26
3.10 X-ray diffraction .....	27
3.11 Optical spectroscopy .....	28
3.12 References .....	28
<b>4 The CdS/CdTe solar cell. Alternative steps of fabrication process</b> .....	<b>29</b>
4.1 Introduction.....	29
4.2 Different CdS growth process .....	29
4.3 Different Bromine-Methanol etching.....	36
4.4 References .....	39

<b>5</b>	<b>Low substrate temperature deposited CdTe solar cells with an alternative recrystallization process .....</b>	<b>41</b>
5.1	Abstract .....	41
5.2	Introduction .....	42
5.3	Solar cells fabrication.....	42
5.3.1	<i>TCO substrate.....</i>	42
5.3.2	<i>CdS deposition and post-deposition treatment .....</i>	43
5.3.3	<i>CdTe deposition and post-deposition treatment .....</i>	43
5.4	Activation treatment.....	44
5.4.1	<i>CdCl<sub>2</sub> treatment.....</i>	44
5.4.2	<i>Freon treatment.....</i>	44
5.5	Morphological Analysis .....	45
5.6	XRD Analysis .....	48
5.7	Back contact.....	52
5.8	Performance .....	52
5.9	Conclusions .....	54
5.10	References.....	55
<b>6</b>	<b>Influence of CdTe thickness on structural and electrical properties of CdTe/CdS solar cells .....</b>	<b>57</b>
6.1	Abstract .....	57
6.2	Introduction .....	58
6.3	Experimental details.....	58
6.4	Results and Discussion.....	59
6.4.1	<i>Morphology of CdTe.....</i>	59
6.4.2	<i>X-ray diffraction of CdTe layers.....</i>	62
6.5	Solar cell devices.....	66
6.6	Conclusions .....	68
6.7	References.....	69
<b>7</b>	<b>Flexible CdTe solar cells by a low temperature process on ITO/ZnO coated polymers.....</b>	<b>71</b>
7.1	Abstract .....	71
7.2	Introduction .....	72
7.3	Experimental details.....	73
7.4	Results and discussion.....	74
7.4.1	<i>Layer and Device Characterization.....</i>	74
7.4.2	<i>Laser scribing.....</i>	79
7.5	Conclusions .....	81
7.6	References.....	82

<b>8</b>	<b>Final conclusions.....</b>	<b>85</b>
	<b>List of abbreviations .....</b>	<b>87</b>
	<b>Acknowledgments .....</b>	<b>89</b>
	<b>List of publications.....</b>	<b>91</b>
	<b>Curriculum vitae .....</b>	<b>93</b>



## Summary

Presented in this thesis are the results from the study of new fabrication approaches for high efficiency thin film CdS/CdTe solar cells grown in superstrate configuration. Hereinafter the phrases CdS/CdTe solar cells and thin film CdS/CdTe solar cell will imply thin film CdS/CdTe solar cell grown in superstrate configuration.

This thesis contains four main parts. The first part (chapters 1 and 2) presents general information about thin film CdS/CdTe solar cells, and their place among other types of solar cells. A definition of the device is given and explained. Possible configurations of thin film CdS/CdTe solar cells are shown. A historical overview of the evolution of thin film CdS/CdTe solar cell efficiency from 1969 - advent of the first thin film CdS/CdTe solar cell – up to now is presented. A short overview of the main ongoing research and present challenges is given in the paragraph “Current research directions”. Also included in this section is the aim of this study defined according to present-day challenges for CdTe photovoltaic.

In the second part (chapter 3) the fabrication process for thin film CdS/CdTe solar cells preparation developed in our laboratory by the author is presented. All steps starting from substrate up to the finished working device are mentioned. All the required techniques and materials are specified. Moreover in the second part the experimental techniques, which were used for solar cells characterization, are presented. The operating modes for each type of characterization are also presented.

The third part (from chapter 4 to chapter 7) focuses on the new fabrication approaches for thin film CdS/CdTe solar cells. Influence of alternative fabrication steps in lieu of our standard fabrication process steps on solar cells performance is presented. We examined how the performance of CdS/CdTe solar cells is influenced by: different fabrication methods of CdS window layer and different Bromine-Methanol etching.

An alternative recrystallization process for low substrate temperature deposited CdTe solar cells was studied. The influence of alternative treatment on CdS/CdTe solar cells behavior and performance is presented. Results are compared with the results from the standard process.

Results of the study addressed by tellurium scarcity are presented in chapter 5. Influence of CdTe thickness on structural and electrical properties of CdTe/CdS solar cells was investigated.

In chapter 7 flexible solar cells production process developed in our laboratory is presented. Results and challenges addressed by the fabrication of flexible CdTe solar cells by a low temperature process on ITO/ZnO coated polymers are presented in this chapter.

In the fourth part all results obtained during this study are summarized and presented. The results have already been partly published in peer-reviewed journals and conferences proceedings.

# 1 Introduction

## 1.1 Thin film CdS/CdTe solar cells

A solar cell (also called photovoltaic cell) is a solid state device that converts the sunlight energy directly into electricity by the photovoltaic effect. Energy conversion is based on the theory of p-n junction: free carriers (electrons and holes) generated by sunlight absorption are separated by the p-n junction and finally extracted in the external circuit.

Among the different technologies the most important ones are monocrystalline and polycrystalline silicon solar cells, amorphous silicon solar cells, cadmium telluride and copper indium gallium diselenide (CIGS) thin film solar cells. In these single-junction solar cells one of the two semiconductors forming the p-n junction has suitable value of the band gap in which sunlight is absorbed [1]. If p-n junction is made from differently doped layers of the same semiconductor material it is called homojunction. Silicon based monocrystalline and polycrystalline solar cells are homojunction solar cells. Heterojunctions are p-n junction made with two different types of semiconductors with unequal band gaps: CdTe and CIGS cells are heterojunction solar cells.

Thin film solar cell can be defined as a device, which consists of layer sequence from disordered semiconductor materials that are deposited onto a supporting substrate or superstrate. In thin film solar cells the number of functional layers can amount to up to eight and more [2]. Thin film solar cells, with their relatively high efficiency and lower energy cost - almost comparable with usual energy sources - are one of the most promising type of solar cells [3].

CdS/CdTe thin films solar cell is a heterojunction device with CdS as window layer and CdTe as absorber layer. Those layers are very thin (below 10  $\mu\text{m}$ ) and have a polycrystalline nature both for CdS and CdTe. Schematic energy-band diagram of the CdS/CdTe thin film solar cell under light is presented in figure 1.1 [4].

CdTe is a semiconductor with a direct band gap of (1.47 – 1.5) eV [5, 6], this is an optimum value for converting sunlight into electricity [1]. CdTe has a high absorption coefficient: 2  $\mu\text{m}$  CdTe layer is enough to absorb most of the sunlight [6]. This layer can be produced by physical vapour deposition (PVD) methods: closed space sublimation (CSS) [7], vacuum evaporation (VE) [8].

CdS is a semiconductor with a direct band gap of (2.42 - 2.5) eV [5, 6]. It is used as window layer transmitting wavelengths above 510 nm or lower, if the layer is thinner. However in very thin CdS layers pinholes can appear because of inhomogeneity of the film or because of the consumption of CdS during activation treatment. For CdS deposition VE [9], chemical bath deposition (CBD) [9] and sputtering [10] can be used.

Different transparent conductive oxide (TCO) films can be used as front contact: indium tin oxide (ITO), fluorine tin oxide (FTO), zinc oxide doped with aluminium (Al:ZnO). The most important requirements for front contact are to be transparent (to allow photons to reach the p-n junction) and to have high conductivity (to collect the photogenerated current). Sputtering is typically used for deposition of the front contact [11].

Also the back contact is necessary to collect the current. The most used contact is Cu-Au bilayer, which allows having an ohmic back contact, despite the high electron affinity of CdTe. It is necessary to say that it is not easy to make good ohmic back contact for CdTe because of the barrier given by high electron affinity and band gap [6]. For the deposition of the back contact different PVD methods can be used, among them sputtering and vacuum evaporation. After the deposition of back contact it is necessary to make annealing of the last for diffusion of copper into CdTe layer in order to dope it [12]. To enhance this diffusion the solar cell is usually heated in air atmosphere.

CdTe needs a post deposition treatment (also called activation process, activation treatment,), which improves dramatically the electrical properties (carriers concentration, conductivity) of the film. Usually the activation treatment is made by a reaction between  $\text{CdCl}_2$  and CdTe at a temperature of 400 °C. During this process, grains of CdTe become larger, the defect density at the junction decrease and grain boundaries are passivated. Last but not least: during the treatment  $\text{CdS}_x\text{Te}_{1-x}$  intermixed layer is formed due to sulfur diffusion into CdTe [6].

Thin film CdS/CdTe solar cells can be grown in substrate and superstrate configuration. The structure of the solar cell in superstrate configuration is glass/front contact/CdS/CdTe/back contact (see figure 1.2). Sunlight, before reaching the p-n junction, will pass through the glass, front contact, CdS and then absorbed by CdTe. For superstrate configuration the fabrication process starts from the deposition of the front contact on the transparent substrate (usually glass). Then sequentially CdS window layer and CdTe absorber layer are deposited. And finally back contact is formed after the activation of CdTe.

In case of substrate configuration thin film CdS/CdTe solar cell (figure 1.2) is fabricated in opposite way. Fabrication starts from deposition of the back contact on the substrate, which does not need to be transparent in this case. Then sequentially CdTe absorber layer and CdS window layer are deposited. Activation treatment can be applied after CdTe deposition or after CdTe and CdS depositions. Finally front contact is formed on CdS window layer [13].

The direct band gap of 1.45 eV, and high absorption coefficient,  $> 5 \times 10^5/\text{cm}$ , of CdTe means that high quantum yield can be expected over a wide wavelength range, from the ultraviolet to the CdTe band gap,  $\lambda \sim 825$  nm. The high CdTe absorption coefficient,  $> 5 \times 10^5/\text{cm}$ , for photons with  $E > E_g$  translates into 99% absorption of the absorbable AM1.5 photons within 2  $\mu\text{m}$  of film thickness. The theoretical solar cell efficiency for thin film CdTe solar cells is around 28 % [6].

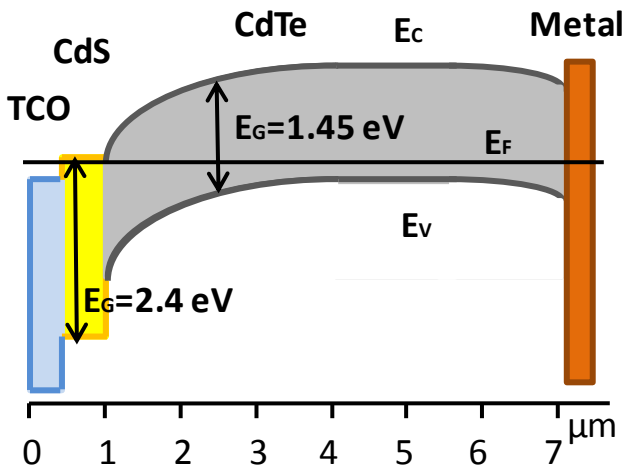


Figure 1.1: Schematic energy band diagram for CdS/CdTe thin film solar cell.

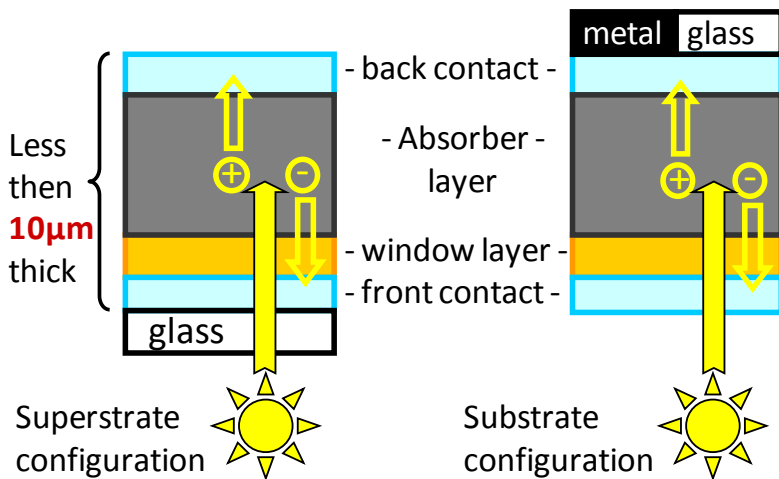


Figure 1.2: Basic structures of CdS/CdTe solar cells.

Advantages of CdS/CdTe thin film solar cells are: simple and cheap fabrication process, high scalability and small amount of required materials. This result in reduction of production cost down to 0.67 \$ per watt by November 2012 [14].

## 1.2 Historical overview of CdTe photovoltaic

History of CdTe starts in 1969 when Russian's scientists E. I. Adirovich, Y. M Yuabov and G. R Yagudaev presented thin film CdTe solar cell in superstrate configuration. CdTe film was deposited by evaporation on CdS/SnO<sub>2</sub>/glass stack, and the solar cell performed efficiency around 2 % [6]. It was a prophetic article: nowadays this configuration is considered as a "standard" or "usual" one, all commercial products follow this configuration [15].

The first attempts to commercialize CdTe PV modules were initiated in the early 1980's by the Japanese company Matsushita (CdTe record holder from 1976 to 1980 [16]) by producing CdTe cells using a low-cost screen printing process [17].

Monosolar (obtained CdTe record in 1980 [16]) and Ametek (obtained CdTe record in 1988 [16]) were developing an electrodeposition process for CdTe solar cells. After them Photon Energy made the biggest progress in CdTe technology with their low-cost wet-chemicals methods of deposition [17]. Photon Energy obtained CdTe world record in 1989 with a 12.3 % efficiency solar cell with an area of 0.302 cm<sup>2</sup> [18].

In 1991 a group from University of South Florida presented a new record solar cell of 1 cm<sup>2</sup> area with an efficiency of 13.4 %. The record CdS/CdTe solar cell has been prepared on fluorine-doped tin oxide-coated glass (SnO<sub>2</sub>:F/glass) substrate using CdS film grown from an aqueous solution and p-CdTe film deposited by CSS [19]. The optimization of the fabrication process by reducing the CdS thickness, the back contact optimization and the application of antireflection (AR) coating result in new records: CdTe solar cell with efficiency of 14.6 % was presented in 1992 [20] and then, in 1993, efficiency of 15.8 % with 1.05 cm<sup>2</sup> CdTe solar cell was achieved [7] (parameters of record cells are presented in table 1.1).

The record efficiency was renewed in 1997 by H. Ohyama et al. from Matsushita Battery Industrial Co. Ltd. from Japan [21]. Solar cells were made depositing ITO film by sputtering on borosilicate glass, then very thin (50 nm) CdS film was formed by metal organic chemical vapor deposition (MOCVD), CdTe film was formed by CSS and activated by wet CdCl<sub>2</sub> treatment; finally, carbon and silver electrodes were fabricated by a screen printing and sintering method, which results in record efficiency of 16 % [22]. The key for this record was the high current density of the device provided by ultra thin (50 nm) CdS layer made by MOCVD (see table 1.1).

Table 1.1: Record efficiencies of CdS/CdTe solar cells.

Eff., %	Voc, mV	FF, %	Jsc, mA/cm <sup>2</sup>	Area, cm <sup>2</sup>	Made by	AR coating
13.4	840	72.6	21.9	1	UoSF	None
14.6	850	70.4	24.4	1.08	UoSF	MgF <sub>2</sub>
15.8	843	74.5	25.1	1.05	UoSF	MgF <sub>2</sub>
16.0	840	73.1	26.1	1.0	Matsushita	MgF <sub>2</sub>
16.4	848	74.5	25.9	1.131	NREL	MgF <sub>2</sub>
16.5	845	75.5	25.9	1.032	NREL	MgF <sub>2</sub>
17.3	842	75.6	27.2	1.066	First Solar	No data
18.3	857	79	26.95	1.005	GE	No data
18.7					First Solar	No data

In 2001 a group from National Renewable Energy Laboratory (NREL), reported record efficiencies of CdS/CdTe solar cells above 16 %. This improvement was achieved by modifying SnO<sub>2</sub>/CdS/CdTe device structure “used for more than 30 years” [23] substituting SnO<sub>2</sub> front contact with cadmium stannate (Cd<sub>2</sub>SnO<sub>4</sub> or CTO) transparent conductive oxide and integrating the high-resistivity zinc stannate (Zn<sub>2</sub>SnO<sub>4</sub> or ZTO) buffer layer into CdTe cells [23]. These investigations resulted in two following record CdTe solar cells from NREL: 1.131 cm<sup>2</sup> area cell with efficiency of

16.4 % in 2001 [24] and then, in the same 2001 1.032 cm<sup>2</sup> area cell with efficiency of 16.5 % [23, 25]. This record stands for ten years.

The year 1999 was a very important year for CdTe photovoltaics. First Solar, Inc. in United States and Q-Cells in Germany (promoters of Calyxo) were founded - the main producers of CdTe modules at present with capacity of 1900 MW/year and 85 MW/year respectively [26, 27]. In 2011, after long 10 years from previous record First Solar presented the 1.066 cm<sup>2</sup> solar cell with efficiency of 17.3 % [28]. Cell's performance was improved by increasing the current density compared with previous record from Wu (see table 1.1).

At the end of the 2012 General Electric (GE) Company presented the new record – 18.3 % for 1.005 cm<sup>2</sup> CdTe solar cell [29].

At the beginning of the 2013 when this thesis was written First Solar presented new record solar cell with efficiency of 18.7 % [30]. CdTe module record (14.4 % at 6750.9 cm<sup>2</sup>) is also owned by First solar [28].

### 1.3 Current research directions

Thin film CdTe solar cells have reached efficiency of 18.7 % for a 1 cm<sup>2</sup> solar cell (look previous paragraph) and 14.4 % for a solar module [30]. This high scalability together with cheap and simple fabrication process allowed CdTe to reach 5 % of the photovoltaic market in 2011. But still there are challenges for CdTe photovoltaic.

Apart from increasing CdTe solar cell efficiency other important research issues are pursued: development of an effective and stable back contact, CdTe thickness reduction, deep understanding of the activation treatment.

Despite CdTe photovoltaic already arrived to successful industrial production, there are ongoing researchs of stable back contact for CdTe, which would show ohmic behaviour. One of the possible solutions is Sb<sub>3</sub>Te<sub>2</sub> back contact developed by N. Romeo et al. Efficiencies exceeding 14 % were achieved with mentioned back contact made by radio frequency sputtering [31].

J. M. Burst et al., studied the use of ZnTe:Cu as a back contact for CdTe grown at temperatures up to 620 °C. They observed that CdTe solar cells with absorber layers deposited by CSS at high temperature, 600 – 620 °C, are steadier and more persistent to the contacting temperature than CdTe grown at lower temperatures, 550 °C. Also it was observed a ~1 % absolute increase in device efficiency for devices in which the CdTe is deposited on PV glass at high temperature [32].

A. Jarkov et al. prepared a polypyrrole back contact by electrodeposition for a CdS/CdTe solar cells structure prepared by high vacuum evaporation. Performance of complete solar cell structures with polypyrrole back contact is comparable with performance of the same structures with conventional Cu containing back contact. [33].

MoO<sub>x</sub> buffer layer is possible material, which allowed producing stable back contact. It was showed by Lin et al. that with MoO<sub>x</sub> as the back contact buffer, various metals with different work functions can be used as the back contact electrode to achieve relatively high efficiencies. Solar cells with high work function metals including Ni and Mo as the back electrode show better stability compared to those with low work function metals such as Al [34, 35].

Another challenge for CdTe photovoltaic is Te scarcity, as far as it is rare element. These force researchers to look for possible solutions of this problem. One of the possibilities is to decrease CdTe thickness and therefore to reduce amount of Te needed for each module.

N. R. Paudel et al. presented a work where they have prepared thin film CdS/CdTe cells with CdTe thickness from 0.25 μm to 2.1 μm by magnetron sputtering. They obtained 8 % efficiency with only 0.25 μm of CdTe and 11 % efficiency with 0.5 μm with cells area of 0.06 cm<sup>2</sup> [36].

V. K. Krishnakumar et al. suggested to use double CdTe layer in order to avoid formation of pinholes during CdTe deposition. Dividing CdTe formation process in two steps allowed them to get rid of shunts [37].

Another important topic is the use of CdCl<sub>2</sub> to be considered a toxic material which is used in the CdTe fabrication process. A

possible solution is the substitution of  $\text{CdCl}_2$  with another non-toxic chemical.

J. Türck et al. suggested  $\text{ZnCl}_2$  as an alternative for  $\text{CdCl}_2$ . They showed the possibility to produce CdS/CdTe thin film solar cells just substituting  $\text{CdCl}_2$  with  $\text{ZnCl}_2$  in wet activation treatment; however solar cell's efficiency was less than 9 % [38].

A group from the University of Toledo presented photochemical pyrrole based treatment developed in their laboratory. Aqueous solutions containing pyrrole and sodium chloride provide a treatment of the CdTe surface when the device is illuminated with visible light resulting in efficiency of 12.3% [39].

A. Rios-Flores et al. presented CdS/CdTe solar cell with 14.6 % efficiency activated with  $\text{HCF}_2\text{Cl}$  gas treatment. Advantage of this process is that activation treatment getting rid of  $\text{CdCl}_2$  became all in vacuum activation process [40]. This result is continuation of the work of N. Romeo, who first substituted  $\text{CdCl}_2$  with a non toxic gas such as Freon [41].

Last but not least is the research of CdTe solar cells grown in substrate configuration. It is one of the promising directions for CdTe photovoltaic because for this configuration performance of the cells does not affected by substrate as for superstrate case. It was shown that CdTe solar cells in substrate configuration could reach efficiency exceeding 10 % [42]. Good results were provided by C. Gretener et al. [13] and by R. G. Dhere et al. [43] but this issue is out of the scope of this thesis.

## 1.4 References

- [1] W. Shockley and H. J. Queisser, J. Appl. Phys. 32, 510 (1961); doi: 10.1063/1.1736034.
- [2] D. Abou-Ras, T. Kirchartz, U. Rau, Advanced Characterization Techniques for Thin Film Solar Cells, 2011 WILEY-VCH Verlag GmbH & Co. KGaA.

- [3] GBI Research, Thin Film Photovoltaic PV Cells Market Analysis to 2020 CIGS Copper Indium Gallium Diselenide to Emerge as the Major Technology by 2020, GBIAE0010MR, 2010.
- [4] J. Pan, M. Gloeckler, L. R. Sites, *J. Appl. Phys.* 100, (2006) 124505.
- [5] Singh J, *Physics of Semiconductors and Their Heterostructures*, 1993, McGraw-Hill.
- [6] B. E. McCandless and J. R. Sites, *Handbook of photovoltaic Science and Engineering*. Edited by A. Luque and S. Hegedus © 2003 John Wiley & Sons, Ltd ISBN: 0-471-49196-9.
- [7] J. Britt and C. Ferekides, *Appl. Phys. Lett.* 62 (22), 31 May 1993, 2851-2852.
- [8] A. Romeo, D.L. Batzner, H. Zogg, A.N. Tiwari, *Thin Solid Films* 361-362 (2000) 420-425.
- [9] A. Romeo, D.L. Batzner, H. Zogg, C.Vignali, A.N. Tiwari, *Solar Energy Materials&Solar Cells* 67 (2001) 311-321.
- [10] A. D. Compaan, A. Gupta, S. Lee, S. Wang, J. Drayton, *Solar Energy* 77 (2004) 815-822.
- [11] N. Romeo, A. Bosio, R. Tedeschi, A. Romeo, V. Canevari, *Solar Energy Materials & Solar Cells* 58 (1999) 209-218.
- [12] T. A. Gessert, S. Smith, T. Moriarty, M. Young, S. Asher, S. Johnston, A. Duda, C. DeHart, A. L. Fahrenbruch, 2005, NREL/CP-520-36472.
- [13] C. Gretener, J. Perrenoud, L. Kranz, L. Kneer, R. Schmitt, S. Buecheler and A. N. Tiwari, *Prog. Photovolt: Res. Appl.* (2012) DOI: 10.1002/pip.2233.
- [14] <http://investor.firstsolar.com>, First Solar Q3 Earnings Presentation, First Solar, November 1, 2012.
- [15] Thin film solar module CX3 specification, <http://www.calyxo.com/en/product/module-cx3.html>.
- [16] [http://www.nrel.gov/ncpv/images/efficiency\\_chart.jpg](http://www.nrel.gov/ncpv/images/efficiency_chart.jpg).

- [17] T. B. Johansson, *Renewable energy: sources for fuels and electricity*, 1993, Island Press.
- [18] S. P. Albright, J. F. Jordan, B. Ackerman, R.R. Chamberlin, *Solar Cells*, Volume 27, Issues 1–4, October–December 1989, Pages 77-90.
- [19] T. L. Chu, S. S. Chu, C. Ferekides, C. Q. Wu, J. Britt, and C. Wang, *J. Appl. Phys.* 70 (12), 15 December 1991, 7608-7612.
- [20] T. L. Chu, Shirley S. Chu, J. Britt, C. Ferekides, C. Wang, C. Q. Wu, and H. S. Ullal, *IEEE ELECTRON DEVICE LETTERS*. VOL. 13, NO. 5. MAY 1992, 303-304.
- [21] M. A. Green, K. Emery, K. Bucher, D. L. King and S. Igari, *Prog. Photovolt. Res. Appl.*, 5, 265-268 (1997).
- [22] H. Ohyama, T. Aramoto, S. Kumazawa, H. Higuchi, T. Arita, S. Shibutani, T. Nishio, J. Nakajima, M. Tsuji, A. Hanafusa, T. Hibino, K. Omura and M. Murozono, *IEEE*, 26th PVSC, 1997, 343-346.
- [23] X. Wu, R. G. Dhere, D. S. Albin, T. A. Gessert, C. DeHart, J. C. Keane, A. Duda, T. J. Coutts, S. Asher, D. H. Levi, H. R. Moutinho, Y. Yan, T. Moriarty, S. Johnston, K. Emery, and P. Sheldon, report NREL/CP-520-31025, October 2001.
- [24] M. A. Green, K. Emery, D. L. King, S. Igari and W. Warta, *Prog. Photovolt: Res. Appl.* 2001; 9:287-293.
- [25] X. Wu, *Solar Energy* 77 (2004) 803–814.
- [26] <http://www.renewindians.com/2012/08/first-solar-to-increase-module.html>.
- [27] <http://www.calyxo.com/en/news-events/news/114-calyxo-gmbh-increases-capacity-to-85-mw.html>.
- [28] M. A. Green, K. Emery, Y. Hishikawa, W. Warta and Ewan D. Dunlop, *Prog. Photovolt: Res. Appl.* 2012; 20:606–614.
- [29] M. A. Green, Personal communication.

- [30] Press relies from First solar, 26 February 2013, <http://investor.firstsolar.com/releasedetail.cfm?ReleaseID=74339>.
- [31] N. Romeo, A. Bosio, R. Tedeschi, V. Canevari, *Materials Chemistry and Physics* 66 (2000) 201-206.
- [32] J. M. Burst, W. L. Rance, T. M. Barnes, M. O. Reese, J. V. Li, D. Kuciauskas, M. A. Steiner, T. A. Gessert, K. Zhang, C.T. Hamilton, K. M. Fuller, B. G. Aitken, and C. A. Kosik Williams, 37th IEEE, pages 000188-000191, 2011.
- [33] A. Jarkov, S. Bereznev, O. Volobujeva, R. Traksmaa, A. Tverjanovich, A. Opik, E. Mellikov, *Thin Solid Films*, Available online 31 January 2013.
- [34] H. Lin, Irfan, W. Xia, H. N. Wu, Y. Gao, C. W. Tang, *Solar Energy Materials & Solar Cells* 99 (2012) 349–355.
- [35] I. Irfan, H. Lin, W. Xia, H. N. Wu, C. W. Tang, Y. Gao, *Solar Energy Materials & Solar Cells* 105 (2012) 86–89.
- [36] N.R. Paudel, K.A. Wieland, A.D. Compaan, *Solar Energy Materials & Solar Cells* 105 (2012) 109–112.
- [37] V. K. Krishnakumar, A. Barati, H.-J. Schimper, A. Klein and W. Jaegermann, 27th EU PVSEC, 2012, Visual presentation.
- [38] J. Türeck, A. Schnikart, H.-J. Schimper, A. Klein and W. Jaegermann, 27th EU PVSEC, 2012, Visual presentation.
- [39] D. K. Koll, A. H. Taha, D. M. Giolando, *Solar Energy Materials & Solar Cells* 95 (2011) 1716–1719.
- [40] A. Rios-Flores, O. Ares, J. M. Camacho, V. Rejon, J. L. Pena, *Solar Energy* 86 (2012) 780–785.
- [41] N. Romeo, A. Bosio, A. Romeo, S. Mazzamuto and V. Canevari, 21st EU PVSEC, 2006, pages 1857-1860.
- [42] N. Romeo, A. Bosio, S. Mazzamuto, D. Menossi, J. L. Pena, A. Salavei, I. Rimmaudo, V. Allodi, A. Romeo, *Proceedings of the 26th EU PVSEC* 2011.

- [43] R. G. Dhere, J. N. Duenow, C. M. DeHart, J. V. Li, D. Kuciauskas, and T. A. Gessert, NREL/CP-5200-54126.



## 2 Aim of this work

The goal of this project is to study new fabrication approaches for high efficiency CdS/CdTe solar cells. This includes the following steps:

- a fabrication process based on low temperature PVD methods should be developed for successful preparation of high efficiency thin film CdS/CdTe solar cells in superstrate configuration. This includes the study of different process steps influence on properties of solar cells and initial device optimization to establish a “standard” solar cell fabrication process in order to improve the performance of CdS/CdTe solar cells.

- in order to substitute the CdCl<sub>2</sub> activation treatment an alternative activation process for CdS/CdTe solar cells should be suggested and its influence on the CdS/CdTe solar cells performance should be studied.

- an effect of CdTe thickness reduction on structural and electrical properties of CdTe/CdS solar cells should be investigated in order to look into the possibility to decrease dramatically the amount of CdTe material needed for fabrication of high efficiency thin film CdS/CdTe solar cells.

- the developed low temperature fabrication process should be applied to flexible substrates in order to produce flexible thin film CdS/CdTe solar cells. The effect of the flexible substrates on the performance of the solar cells should be investigated.

We decided on the above-listed topics as the main research directions for this study due to their challenging character (a detailed review of the current research directions in CdTe field is presented in paragraph 1.3). It is our hope that this work will yield new important results for CdTe photovoltaics.



## **3 The CdS/CdTe solar cell. Fabrication process and characterization**

### **3.1 Introduction**

In this chapter the fabrication process of CdS/CdTe solar cells in superstrate configuration developed in our laboratory is presented. Functional layers are deposited by the means of PVD, using low temperature fabrication process. The maximum temperature during the fabrication process is 450 °C. This process has the advantage that more materials, like polymers, which are stable at this temperature, are available as substrates.

Fabrication steps from the standard process will be compared with alternative methods in chapter 4. A comparison study of the influence of different fabrication steps on performance of thin film CdS/CdTe solar cells is presented.

Hereinafter, we will describe our standard fabrication process, with which we routinely produce thin film CdTe solar cells with efficiency exceeding 14 %.

### **3.2 Substrate**

As far as we make thin-film CdTe solar cells in superstrate configuration the requirements for the substrates are: transparency, chemical stability, mechanical robustness, and low cost. In superstrate solar cell light would first pass through the substrate. In order to collect as much sun light as possible, substrates need to be as transparent as possible to sun-light. Mechanical robustness implies

that the substrate would withstand the fabrication process and at the same time, provide a support for solar cell structure consisting of thin films, which do not possess structure rigidity. Finally the solar cell substrates have to be chemically stable in order to avoid contamination by the diffusion of impurities into the device layers during the deposition steps and, later, in the life cycle of the finished module.

Glass meets the above-mentioned requirements. Usually soda-lime glass or borosilicate (which is more expensive) glass is used as substrates for thin film CdTe solar cells. It is well known that sodium can diffuse from the soda-lime glass and affect the films properties and cell performance. However, it was shown by L. Kranz et al. that a ZnO:Al layer can effectively suppress sodium diffusion from soda-lime glass [1].

In our laboratory we use soda-lime glass as a substrate for superstrate CdTe solar cells in our standard process.

### 3.3 Front contact

A double layer of ITO deposited by direct current magnetron sputtering and zinc oxide (ZnO) deposited by radio frequency sputtering (RF-sputtering) is used as the standard front contact. Thicknesses of the ITO and ZnO films are 400 nm and 100 nm, respectively. Deposition is made in an argon plus oxygen atmosphere. For ITO, 20 standard cubic centimeters per minute (sccm) of Ar and 0.5 sccm of O<sub>2</sub> are used, while for ZnO, the O<sub>2</sub> flux is changed to 3 sccm. Substrate temperature during deposition is 300 °C. The sheet resistance of ITO layer is below 5 Ohm/square. Industrially prepared ITO/ZnO coated glasses are provided by Arendi S.r.l.

We use 30×30 mm glass samples with ITO+ZnO front contact on which we form thin-film CdTe solar cells.

### 3.4 CdS deposition

Substrates - front contact coated glasses are hand-washed in soap-water solution and then boiled in distilled water for 10-20 min. Then samples are cleaned two times in acetone for 5 min and in isopropanol for 5 min two times in an ultrasonic bath. After cleaning, samples are dried with argon.

CdS window layer is deposited by PVD in a vacuum chamber at a vacuum of  $10^{-5}$  mbar provided by rotary and turbomolecular pumps.

Once the vacuum is reached, an annealing of front contact at  $450\text{ }^{\circ}\text{C}$  for 30 min is applied in order to prepare substrate for subsequent deposition of CdS window layer. The samples in the vacuum chamber are heated by halogen lamps, the temperature is measured by a thermocouple, mounted above the substrate holder (see figure 3.1).

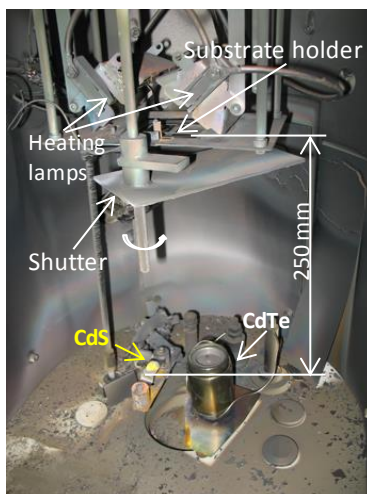


Figure 3.1: Photo of the vacuum chamber where CdS and CdTe are deposited.

Lumps of CdS (99,999 %) are put in a molybdenum boat crucible, which is heated by flowing direct current (DC). During

deposition the substrate temperature is kept at 100 °C. CdS is evaporated with a rate of 0.2-0.7 nm/sec. The thickness of the depositing films is measured in situ with water-cooled piezoelectric quartz measurement system, typically 600 nm of CdS are deposited. After deposition a thermal annealing of CdS films in vacuum at 450°C for 30 min is applied in order to recrystallize CdS and prepare it for following deposition steps.

### 3.5 CdTe deposition

CdTe absorber layer is also deposited by PVD in same deposition chamber (see figure 3.1). High purity CdTe (99.999%) is evaporated by direct heating in a special graphite crucible. Usual deposition rate is in the range of 1 to 3 nm/sec, it is measured in situ with a water-cooled piezoelectric quartz measurement system. Substrate temperature is kept at 340 °C and CdTe film thickness is generally between 6 and 9 µm.

### 3.6 CdCl<sub>2</sub> treatment

Wet CdCl<sub>2</sub> treatment is used for solar cells activation (its role was explained in chapter 1). After deposition of CdS and CdTe, the stacks are blown over with argon and are placed in Petri dish. CdCl<sub>2</sub> solution in methanol is laid on as-deposited CdTe by putting drops of the solution from the pipette in the way that CdTe surface is always wet during the spreading of the solution on CdTe, but at the same time that solution never overflows from the stack of the surface. Then the sample is left in air to let the methanol evaporate and have only CdCl<sub>2</sub> on the surface. This step is made under the laminar flow hood. For our standard process we use 1.5 ml of the solution for a 30×30 mm sample.

The solution recipe: 0.8 grams of CdCl<sub>2</sub> are dissolved in 100 ml of methanol (this refers to 37 % saturated solution [2], [3]) in a glass bottle using a magnetic stirrer (stirred for more than 5 days). Later one part of this saturation solution is mixed with four parts of

methanol. This solution is stirred with a magnetic stirrer for 2 days before use, and it is continuously stirred until its consumption. Hereinafter with “solution” we will refer to the one prepared with the explained recipe.

Front contact areas are cleaned from  $\text{CdCl}_2$  by a watered cotton swab.

As-deposited stacks with  $\text{CdCl}_2$  on top are then thermally treated. The sample in a closed Petri dish is heated in oven in air atmosphere. Our standard treatment is left for 30 min at 410 °C. After treatment the sample is cooled down to room temperature by leaving it in a switched off open oven. Up to 3 samples can be treated simultaneously.

### **3.7 Back contact formation**

Our standard back contact is a stack of copper and gold layers. Cu and Au are grown by PVD in the same vacuum chamber at high vacuum provided by rotary and turbomolecular pumps.

In order to prepare samples for back contact deposition we etch them in bromine-methanol (Br-MeOH) solution. Br-MeOH etching removes the reaction products from the CdTe surface and creates a Te-rich layer. We prepare Br-MeOH solution by putting 0.1 ml of bromine in 40 ml of methanol and stirring to obtain solution with homogeneous color. Under a laminar flow hood the treated sample is immersed in prepared Br-MeOH solution for 40 sec, and then the sample immediately is immersed in isopropanol for 20 seconds to wash off Br-MeOH solution, then the sample is dried with argon.

After Br-MeOH etching, the sample is put in the vacuum chamber (see figure 3.2). For the standard process we use a molybdenum shadow mask, with an array of 0.13 cm<sup>2</sup> round holes.

Copper (99.999 %) and gold (99.99 %) are deposited by vacuum evaporation without heating the sample. After making the vacuum, copper is evaporated from a molybdenum boat crucible, by heating the crucible with DC. Copper deposition is made with a rate in the range of 0.01 to 0.04 nm/sec. The film thickness is measured in situ with a piezoelectric quartz measurement system. Thickness of the

deposited Cu layer in the standard process is 2 nm. Then, without breaking the vacuum, gold is evaporated with the same procedure. Deposition of gold is made with a rate in the range of 0.15 to 0.30 nm/sec. Thickness of the deposited Au layer in the standard process is 50 nm.

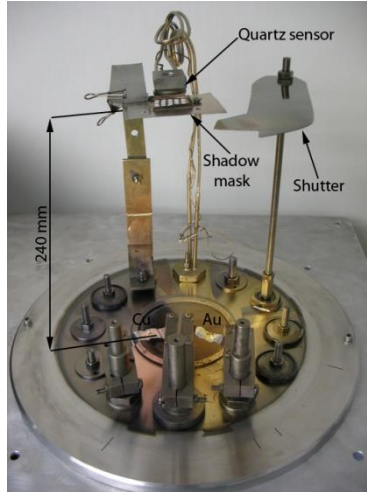


Figure 3.2: Photo of the vacuum chamber where back contact is deposited.

After deposition of Cu and Au the thermal annealing of back contact is made in oven: the sample is heated at 190 °C for 20 min in air.

### 3.8 Current-voltage measurements

Current-voltage measurement (J-V) (current is generally taken as current density) is necessary and sufficient to evaluate the performance of a solar cell. Parameters, obtained from J-V measurement are: open circuit voltage, short circuit current density, current density at the maximum power point and voltage at the maximum power point (see figure 3.3).

Open circuit voltage ( $V_{oc}$ ) is the voltage generated by the illuminated solar cell, when no current flows through the device. It corresponds to the intersection point of J-V characteristic with the x-axis (see figure 3.3).

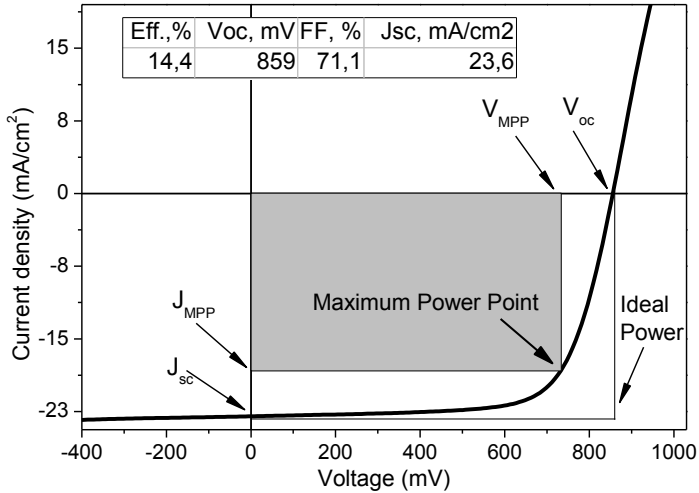


Figure 3.3: Parameters of J-V characteristic under light of a typical solar cell made with the standard process.

Short circuit current ( $J_{sc}$ ) is the current generated by the illuminated device with shorted front and back contacts. It corresponds to the intersection point of the J-V characteristic with y-axis (see figure 3.3).

Current density at the maximum power point ( $J_{MPP}$ ) and voltage at the maximum power point ( $V_{MPP}$ ) define the fill factor as:

$$FF = \frac{V_{MPP} \cdot J_{MPP}}{V_{oc} \cdot J_{sc}} \tag{3.1}$$

Fill factor (FF) is a measure of how close is a solar cell to the ideal current generator or “how square“ it is the J-V characteristic and quantitatively it is the ratio of the maximum power to the ideal power.

The efficiency of solar cell is the ratio of power output to power input (sunlight power) of the cell and can be calculated as:

$$\eta = \frac{P_{\text{output}}}{P_{\text{input}}} = \frac{V_{oc} \cdot FF \cdot J_{sc}}{P_{\text{input}}} \quad (3.2)$$

where  $P_{\text{input}}$  is the incoming irradiance power. The efficiency of the solar cell is the key parameter for defining the ability to convert sun-light into electricity.

The current-voltage characterization of thin-film solar cells is provided with home-made measurement system. We use a halogen lamp to simulate solar spectrum. The halogen lamp is calibrated with silicon photodiode to conform the required conditions of 1000 W/m<sup>2</sup> for a standard characterization. Electrical measurements are made by a Keithley Source Meter 2420We electrometer controlled by software written in LabView. Measurements are made over a bias range from -0.4 V to +1 V with a step size of 0.007 V. Measurements are provided without controlling the sample temperature, but illumination time is shot (around one second), so we consider the heating of the devices as negligible.

### 3.9 Atomic Force Microscopy

Atomic force microscopy (AFM) is used to study morphology of CdS and CdTe films. AFM is a type of scanning probe microscopy with resolution on the order of nanometers. In AFM the information about sample surface is collected by scanning the surface with a mechanical probe. Detailed description of the AFM can be found in textbooks like [4].

The morphological properties of the single layers were studied by AFM with a NT-MDT Solver Pro both in semi-contact and contact mode. Nova software from MT-MDT was used for images acquisition and Image Analysis 3.5 software from NT-MDT was used for generation of 2D and 3D images of the CdS and CdTe

surfaces and extracting information about grains and morphology of the layers.

As-deposited and treated CdTe layers and as-deposited CdS layers were observed by AFM. Typical scans are  $30\ \mu\text{m}\times 30\ \mu\text{m}$ ,  $10\ \mu\text{m}\times 10\ \mu\text{m}$  or  $5\ \mu\text{m}\times 5\ \mu\text{m}$ .

### 3.10 X-ray diffraction

X-ray diffraction analysis (XRD) was used to study crystal structures of CdTe layers. The general use of XRD measurements is to study the difference in the crystal structure of as-deposited and treated CdTe. In case of thin CdTe it is possible to observe CdS and  $\text{CdS}_x\text{Te}_{1-x}$  intermixed layer (see chapter 6).

X-ray diffraction is a non-destructive technique for characterizing crystalline materials. It provides information on structures, phases, preferred crystal orientations, and other structural parameters, such as average grain size and crystal defects. XRD diffraction peaks are produced by interference of a monochromatic beam of x-rays scattered at specific angles from each set of lattice planes in a sample. The peak intensities are determined by the distribution of atoms within the lattice. Consequently, the x-ray diffraction pattern is the unique characteristic of periodic atomic arrangements in a given material [5]. Detailed description of the XRD can be found in textbooks like [5].

Room temperature XRD patterns of the different absorber layers were performed by a Thermo ARL X'TRA powder diffractometer, operating in Bragg-Brentano geometry equipped with a Cu-anode X-ray source ( $K\alpha$ ,  $\lambda = 1.5418\ \text{\AA}$ ) and using a Peltier Si(Li) cooled solid state detector. The instrument setup was the one for thin film measurements. Patterns were collected with a scan rate of  $0.04\ ^\circ/\text{s}$ , time of exposure 1 s and  $2\theta$  range of  $5$  to  $90^\circ$ . The phase identification was performed with the PDF-4+ 2010 database provided by the International Centre for Diffraction Data (ICDD).

### 3.11 Optical spectroscopy

Optical transmission spectra were used to study the transparency of different substrates (glass, polymers), to study how CdS thickness influence the transparency of the film, and to study transparency of thin CdTe layers in order to calculate the band gap of the latest.

Optical transmission measurement refers to spectroscopic techniques that determine the transmission of radiation in optical range through the sample as a function of frequency or wavelength. Transmission spectrum is the intensity of the transmission changes as a function of wavelength [6].

Transmission spectra of our samples are obtained with UNICAM UV/Vis Spectrometer UV2. Unless otherwise specified, measurements are made in air at room temperature at wavelength range of 300 nm - 900 nm with the measurement step of 2 nm.

### 3.12 References

- [1] L. Kranz, J. Perrenoud, F. Pianezzi, C. Gretener, P. Rossbach, S. Buecheler, A. N. Tiwari, *Solar Energy Materials & Solar Cells* 105 (2012) 213–219.
- [2] N. A. Shah, A. Ali, S. Hussain, A. Maqsood, *J. Coat. Technol. Res.*, 7 (1) 105–110, 2010, DOI 10.1007/s11998-008-9146-0.
- [3] W. A. Herrmann, *Synthetic Methods of Organometallic and Inorganic Chemistry*, volume 5, 1999, Thieme Medical Publishers.
- [4] V. J. Morris, A. R. Kirby, A. P. Gunning, *Atomic Force Microscopy for Biologists*, 2012, Imperial College Press.
- [5] D. Abou-Ras, T. Kirchartz, U. Rau, *Advanced Characterization Techniques for Thin Film Solar Cells*, 2011 WILEY-VCH Verlag GmbH & Co. KGaA.
- [6] J. Garcia Solè, and L. E. Bausà, and D. Jaque, *An introduction to the optical spectroscopy of inorganic solids*, 2005, John Wiley & Sons Inc.

## **4 The CdS/CdTe solar cell. Alternative steps of fabrication process**

### **4.1 Introduction**

Thin film CdS/CdTe solar cells in superstrate configuration can be fabricated in different ways, by changing either the structure and/or the fabrication process. In figure 4.1 different structures and fabrication processes for CdS/CdTe solar cell are shown. Different methods of fabrication and different materials for front and back contacts can be chosen.

Alternative to our standard process, presented in chapter 3, we made tests by changing parts of the standard procedure with other frequently used fabrication steps in order to see their influence on performance of our thin film CdS/CdTe solar cells and on the crystallization of the layers.

### **4.2 Different CdS growth process**

Higher current density and higher efficiencies in thin film CdS/CdTe solar cells can be achieved by reducing absorption of the window layer, since CdS has a band gap of 2.4 eV resulting in absorption of wavelengths between 400 and 500 nm [1, 2]. One solution is reducing the CdS thickness. CdS thin films are transparent starting from 510 nm, but with a thickness below 100 nm it is possible to collect light also above 400 nm. From figure 4.2 we observe that 600 nm and 1000 nm thick CdS layers start to transmit light from 510 nm, while CdS layers with thickness of 250 nm and

lower have significant transparency below 510 nm, leading to an increase of produced current.

While thinning the CdS, it is necessary to keep layer homogeneity and a uniform coverage of the TCO in order to avoid pin-holes. Moreover thin CdS needs a high stability to withstand the following depositions and, especially, the CdCl<sub>2</sub> activation treatment, which enhances the diffusion of sulfur into the CdTe consuming the CdS layer [3].

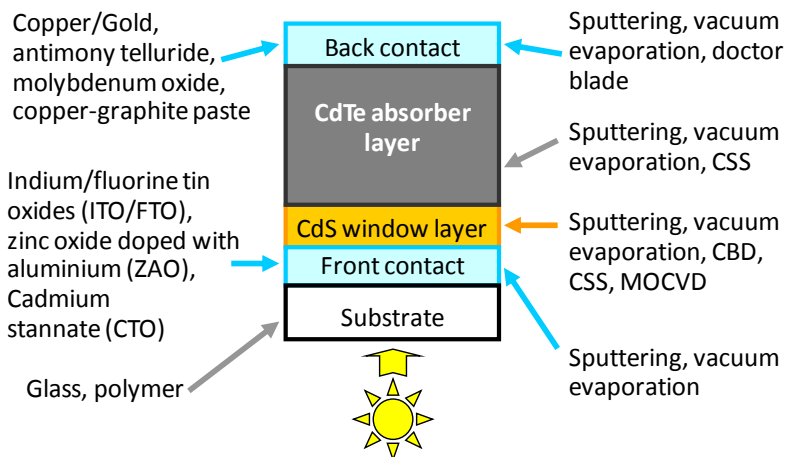


Figure 4.1: Structural and fabrication variations of CdS/CdTe solar cell.

A cadmium sulfide window layer can be grown by different methods: typically CdS is deposited by sputtering [4], vacuum evaporation [5] and chemical bath deposition [6].

Solar cells with window layers made by VE and CBD methods were prepared and compared. CdS layers with thickness of 600 nm were prepared by VE with our standard fabrication process. We also prepared 250 nm thick CdS layers by VE, in order to compare transparency of CdS layers with different thickness and to study the influence on cell performance. The thinner layers, around 80 nm thick, were prepared by CBD. In this case CdS was grown as a

product of the reaction between cadmium acetate  $\text{Cd}(\text{CH}_3\text{COO})_2$ , and thiourea  $\text{CS}(\text{NH}_2)_2$ , in water solution at  $63^\circ\text{C}$  [6, 7].

Atomic force microscopy was used to study the surface morphology of the CdS and CdTe layers. We compared morphology of as-deposited and thermally annealed CdS layers made by VE and CBD and morphology of as-deposited CdTe layers formed on CdS made by CBD and by VE.

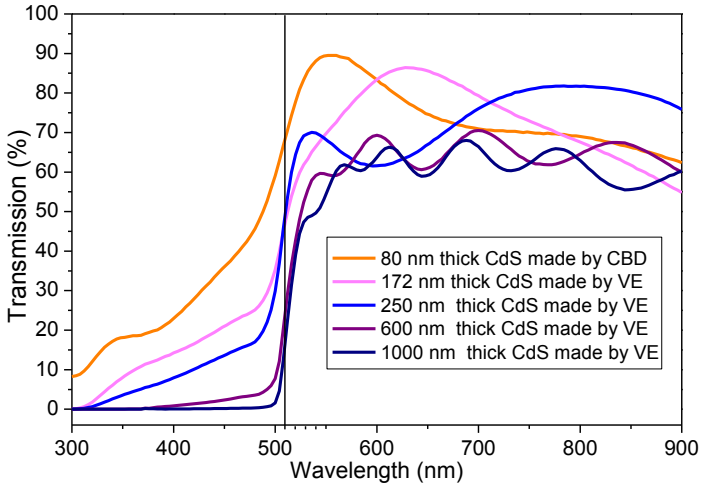


Figure 4.2: Transmission spectra of CdS films of different thickness made by CBD and VE.

In figure 4.3 AFM images of as-deposited CdS layers made by CBD and VE are presented. CdS layers grow in different ways depending on the deposition method. As-deposited CBD CdS layers have a grain size in the range of  $0.1$  to  $0.3\ \mu\text{m}$ . Grains are very similar to each other and the morphology of the film is compact. During the CdS deposition, due to the ongoing reaction between components of the solution, particles form conglomerations that are then deposited on the surface of the sample. As-deposited VE CdS layers have conglomerates in the range of  $0.4$  to  $0.7\ \mu\text{m}$ , which consist of small grains of around  $0.1\ \mu\text{m}$ .

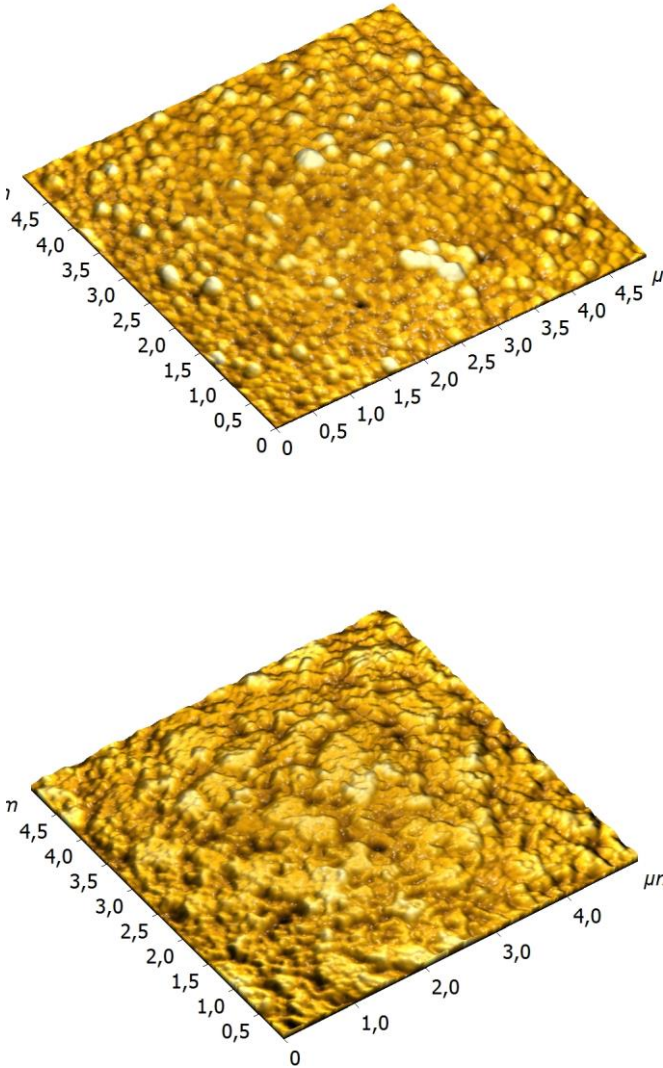


Figure 4.3: AFM images of as-deposited CBD CdS (top) and as-deposited VE CdS (bottom) layers.

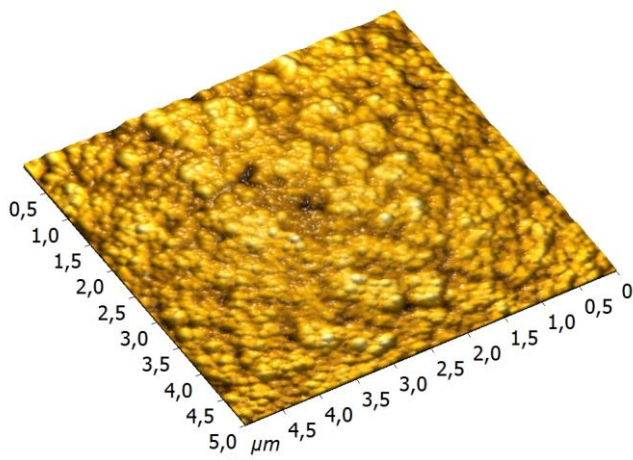
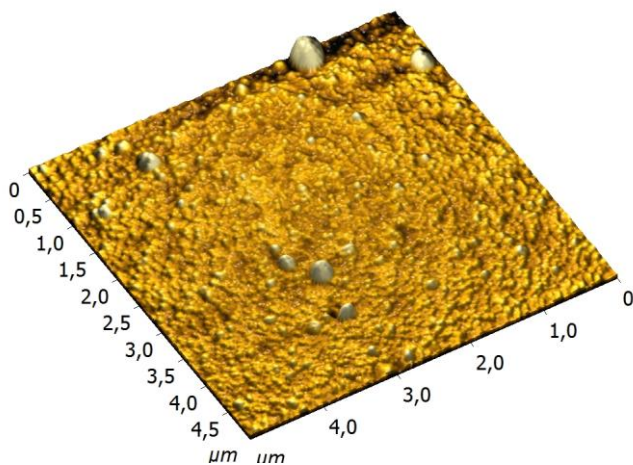


Figure 4.4: AFM images of thermally annealed CBD CdS (top) and VE CdS (bottom) layers.

The morphology of CdS layers changes after thermal annealing made in the vacuum at 450 °C for 30 min (see figure 4.4). In case of CBD CdS grain size decreases down to 0.1 – 0.2  $\mu\text{m}$  while big particles are still present. Annealed layers made by VE are still formed by clusters, which have the same size of the as-deposited case, however small grains have increased their size up to 0.15  $\mu\text{m}$ . Moreover, for VE case, annealed CdS layers have smoother structure than as-deposited ones.

As-deposited CdTe layers show a different morphology due to the different structure of CBD and VE CdS layers (see figure 4.5). The CdTe layers grown on VE CdS show very compact and smooth morphology with similar small grains, their size is in the range of 0.5 to 1  $\mu\text{m}$ . On the other hand, the CdTe grains of the layers grown on CBD CdS have different sizes in the range of 0.5 to 2.5  $\mu\text{m}$  and form a very rough surface.

The performances of CdS/CdTe solar cells with VE and CBD CdS layers were compared. CBD CdS layer has a thickness around 80 nm, while the one made by VE has a thickness of 600 nm. The majority of the solar cells with 250 nm thick VE CdS were shunted probably due to its consumption during the CdCl<sub>2</sub> treatment (as also attested by the lattice parameter calculation, which is presented in chapter 6). Additionally, we observed a degradation of the CdS layers from the glass side, in particular spots and delamination, showing that thin VE CdS layers are not stable to the CdCl<sub>2</sub> activation treatment.

The same problem was observed for CBD CdS that, as mentioned before, were much thinner. Only 30 % of the cells were working in this case.

Solar cells with different CdS window layers show comparable efficiency, however the electrical parameters are different (see figure 4.6). Solar cells with CBD CdS have higher current density compared to cells with VE CdS, but lower  $V_{oc}$  and FF. Higher current density is due to the fact that CdS layers are more transparent (transparency of different CdS window layers is compared in figure 4.2).

Thickness of CBD CdS layer can be a reason for lower  $V_{oc}$  and lower FF. As mentioned before, in thin CdS layer pinholes are easily

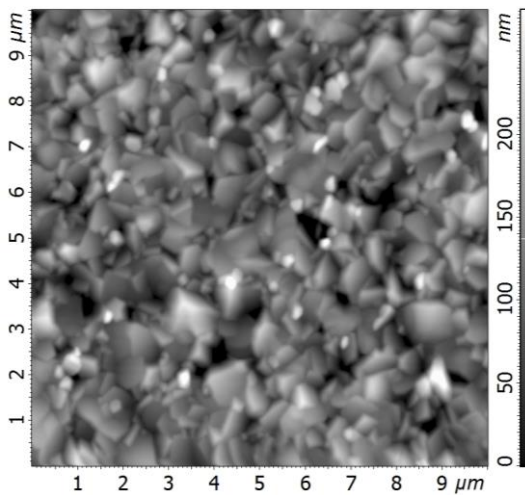
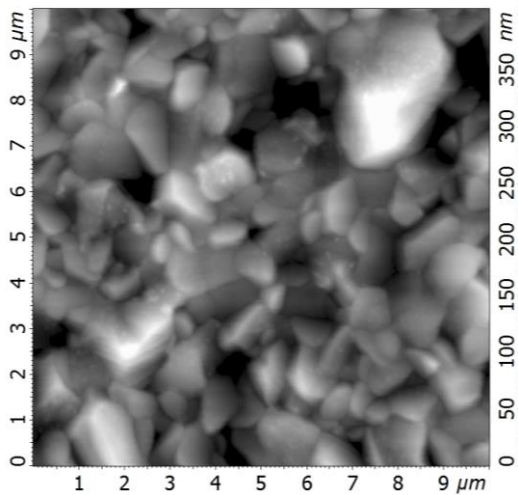


Figure 4.5: AFM images of as-deposited VE CdTe on CBD CdS (top) and on VE CdS (bottom).

generated. This effect is enhanced after  $\text{CdCl}_2$  activation process because of CdS-CdTe intermixing leading to electrical shunts and decreasing  $V_{oc}$  and FF.

Another possible reason for low  $V_{oc}$  and FF is the formation of particles on the substrate as a consequence of the CBD reaction. After CdS deposition these particles would detach from the surface leaving a hole in the layer. These holes in the layer can result in micro shunts and, hence, in reducing of  $V_{oc}$  and FF.

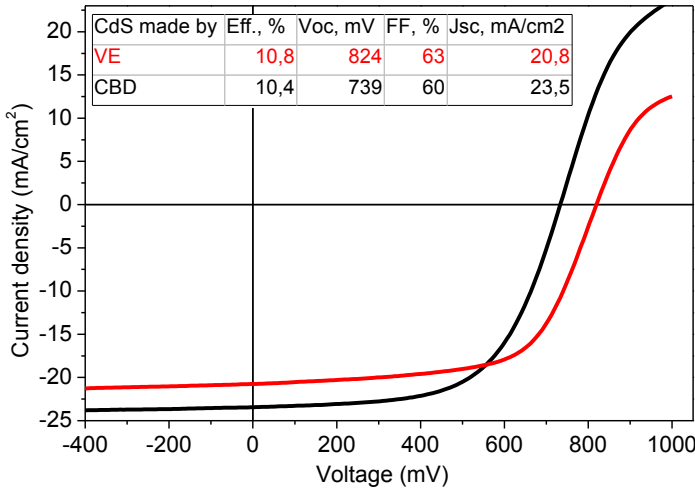


Figure 4.6: I-V characteristics of CdS/CdTe solar cells with CdS window layer made by CBD (black) and made by VE (red).

### 4.3 Different Bromine-Methanol etchings

Ohmic back contact is needed for good performance of the solar cell. But p-type CdTe is a difficult material for making an ohmic back contact, because of the high electron affinity of CdTe, so a high work function (with the value higher than 5.5 eV) metal is needed to make a good ohmic back contact to CdTe [8]. Materials with low work function will form a Schottky contact with reverse biased barrier to the main junction.

Since metals with work function higher than 5.5 eV are rare, the usual solution is to modify the surface of CdTe in order to create a Te rich layer [9]. The modified surface behaves like a p+ semiconductor, decreasing the CdTe work function. This allowed making a quasi-ohmic back contact with some available metals (among them: copper-gold and copper-molybdenum, ZnTe) [8]. Generally, the modification of the CdTe surface is obtained by a wet chemical etching [10].

While studying the stability of solar cells, we were modifying the back contact formation process in order to see how the different etchings influence the stability of the devices.

Copper/gold back contact was deposited by PVD on the CdS/CdTe stacks. Prior to the deposition, Br-MeOH has been applied (see chapter 3 for a detailed explanation).

Br-MeOH etching was modified in two different ways. In one case we changed the etching time: from 40 sec. to 5 sec., followed by standard Cu/Au deposition. In the other case the Br-MeOH etching process was removed and Cu/Au back stacks were deposited on the treated CdTe without cleaning the CdTe surface.

The influence of different etchings on CdTe surface is shown in figure 4.7. On the not etched sample surface, grains of recrystallized CdTe are perfectly visible. Also other particles are present on the surface of CdTe. We consider these residues as products of reactions which take place during the CdCl<sub>2</sub> treatment. The nature of these particles was studied by D.M. Waters et al. [11]. It was discovered that these residues, remaining after the CdCl<sub>2</sub> treatment, contain chlorine compounds like Cd<sub>3</sub>Cl<sub>2</sub>O<sub>2</sub>, which are much more chemically and thermally stable than CdCl<sub>2</sub>. After 5 sec. Br-MeOH etching grains are still visible, but the etching effect of Br-MeOH is obvious – grains are more rounded and have smooth, mirror surfaces. The residue is almost unaffected. The CdTe surface changes dramatically after the standard 40 sec. Br-MeOH etching. No grains or grain boundaries are visible and the surface is very smooth. It is possible to see areas where residue was attached. After the surface modification, cells were finished with our standard back contact.

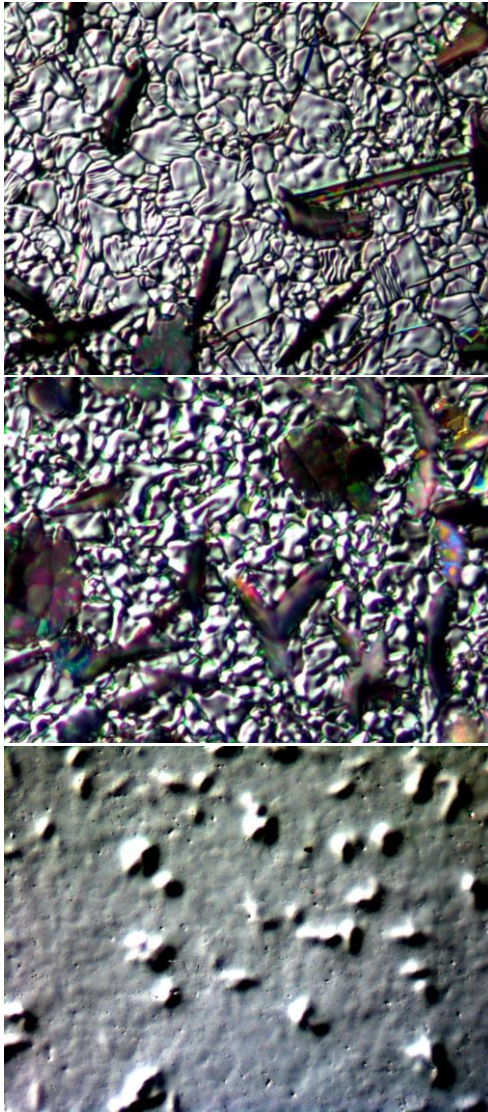


Figure 4.7: Microscope images of treated CdTe surface: without Br-MeOH etching (top), with 5 seconds Br-MeOH etching (middle) and 40 seconds Br-MeOH etching (bottom).

Performance of the finished solar cells was compared. Cells fabricated with Br-MeOH etching step showed very similar behavior (see fig 4.8). Both cells have efficiency exceeding 13 % and in both cases J-V characteristics showed little roll over, which, however does not affect the efficiency of the cells.

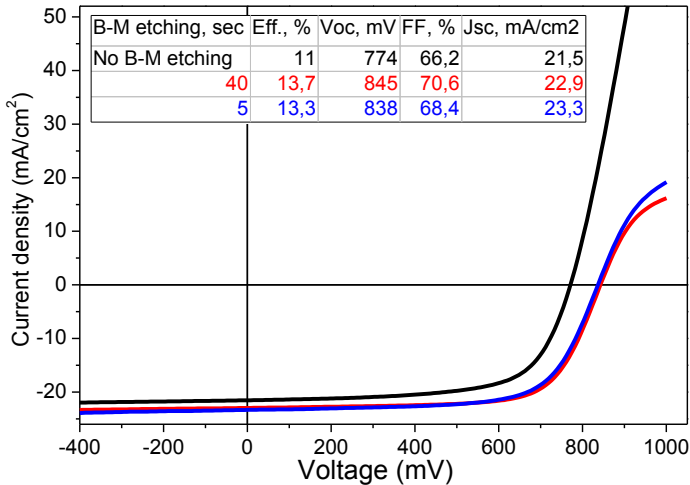


Figure 4.8: I-V characteristics of CdS/CdTe solar cells with 5 sec. (blue), 40 sec. (red) and no (black) bromine-methanol etching.

Solar cell prepared without Br-MeOH etching had efficiency around 11 %. All parameters had lower values compared with cells prepared with Br-MeOH etching. But, surprisingly, J-V characteristics of not etched cells didn't show any roll over.

Solar cells etched with Br-MeOH showed very similar back contact behavior which did not depend on the time of etching. The better back contact was obtained without any etching of CdTe surface but efficiency of the cell significantly decreases.

## 4.4 References

[1] B. E. McCandless and S. S. Hegedus, 1991 IEEE, pages 967-972.

- [2] X. Wu, *Solar Energy* 77 (2004) 803–814.
- [3] R.G. Dhere, Y. Zhang, M.J. Romero, S.E. Asher, M. Young, B. To, R. Noufi, and T.A. Gessert, NREL/CP-520-42567, 2008.
- [4] N. Romeo, A. Bosio, A. Romeo, *Solar Energy Materials & Solar Cells* 94 (2010) 2–7.
- [5] J. Perrenoud, L. Kranz, S. Buecheler, F. Pianezzi, A. N. Tiwari, *Thin Solid Films* 519 (2011) 7444-7448.
- [6] A. Romeo, D.L. Batzner, H. Zogg, A.N. Tiwari, *Thin Solid Films* 361-362 (2000) 420-425.
- [7] A. Romeo, D.L. Batzner, H. Zogg, C.Vignali, A.N. Tiwari, *Solar Energy Materials & Solar Cells*, 67 (2001) 311-321.
- [8] D. L. Batzner, Performance and stability of CdTe/CdS solar cells for terrestrial and space applications, PhD thesis, 2002.
- [9] K. Durose, P.R. Edwards, D.P. Halliday, *Journal of Crystal Growth* 197 (1999) 733-742.
- [10] D.L. Batzner, R. Wendt, A. Romeo, H. Zogg, A.N. Tiwari, *Thin Solid Films* 361-362 (2000) 463-467.
- [11] D.M. Waters, D. Niles, T.A. Gessert, D. Albin, D.H. Rose, and P. Sheldon, 1998, NREL/CP-530-23876.

# **5 Low substrate temperature deposited CdTe solar cells with an alternative recrystallization process**

## **5.1 Abstract**

In this chapter, a CdTe recrystallization process, which avoids the use of CdCl<sub>2</sub>, is presented. In this process CdTe is activated by applying difluorochloromethane gas at a high temperature. This method, called Freon treatment, was introduced successfully for closed space sublimated CdTe (high substrate temperature process) by Romeo et al. [1].

Low substrate temperature process (with a maximum temperature less than 450 °C) was used for solar cells fabrication. CdS and CdTe layers were deposited by thermal evaporation on glass substrates covered with two different front contacts. The alternative activation treatment and usual CdCl<sub>2</sub> treatment were applied during solar cells fabrication. Finally, solar cells were finished with copper/gold back contact.

The structural properties of the CdTe layers activated by different activation steps have been investigated and correlated with photovoltaic properties of the finished devices. Atomic force microscopy and X-ray diffraction analysis showed that the structural properties of CdTe layers depended on underlying substrates and on the type of applied activation treatment. Thin film CdS/CdTe solar cells prepared with low substrate temperature process were less efficient when Freon treatment was used.

This chapter is based on the publications [2, 3].

## 5.2 Introduction

One of the critical steps in fabrication of the high efficiency CdS/CdTe solar cells is the post-deposition heat treatment, also called activation treatment [4]. Usually glass/TCO/CdS/CdTe stacks are treated at high temperature (around 400 °C) in atmosphere of CdCl<sub>2</sub> [5, 6] or with CdCl<sub>2</sub> layer formed by deposition [7] or by immersing glass/TCO/CdS/CdTe stacks into CdCl<sub>2</sub> solution in methanol [8].

Regardless of the fact that CdCl<sub>2</sub> treatment results in high efficient solar cells, toxicity of CdCl<sub>2</sub> forces to look for its appropriate substitution. As it was already shown in chapter 1, the search for suitable replacement for CdCl<sub>2</sub> is important for industrial application. One of the possible solutions is Freon treatment. Freon® (DuPont brand name Freon®, later Freon) is an organic compound that contains carbon, chlorine, hydrogen and fluorine. It is produced as a volatile derivative of methane and ethane. It was shown by N. Romeo et al., that Freon gas could be used in a post-deposition heat treatment instead of CdCl<sub>2</sub> [1]. Efficiency exceeding 15 % was achieved for CdS/CdTe solar cell. In that case CdTe absorber layers were made by high substrate temperature CSS.

Influence of Freon treatment on the thin film CdS/CdTe solar cells made by low substrate temperature deposition was studied and compared with results achieved with CdCl<sub>2</sub> treatment.

## 5.3 Solar cells fabrication

Solar cells were fabricated by depositing each single layer (except for the front contact), namely CdS, CdTe and back contact, by vacuum evaporation.

### 5.3.1 TCO substrate

Two different types of the front contact have been used:

- Commercially available ITO film coated glass with a SiO<sub>2</sub> barrier layer

- Laboratory scale bi-layer of conductive ITO + thin insulating ZnO, deposited at high temperature.

The first one is an ITO deposited by PGO Company, using RF sputtering with the thickness of 180 nm and sheet resistance of 10 Ohm/square.

The second one is a 400 nm ITO+100 nm intrinsic ZnO deposited by RF-sputtering at a temperature of 400 °C with a sheet resistance below 5 Ohm/square. This resulted to be more stable.

### **5.3.2 CdS deposition and post-deposition treatment**

CdS was deposited on the glass/TCO stacks at the substrate temperature of 150 °C using the procedure explained in chapter 3.

CdS layers have been studied in order to increase their stability to the subsequent depositions and the activation treatment of CdTe layer. As a matter of fact one of the limitations that we have been encountered was the diffusion of sulfur into the CdTe that used to be too high, as shown by quantum efficiency measurement (not shown here).

Initially CdS was treated just by heating in vacuum for 30 minutes, leading to a recrystallization of the layer: an enlargement of the grain size from 50-100 nm to 100-200 nm was observed by AFM technique.

However, a different recrystallization treatment was delivered by annealing the CdS at a much higher temperature: in order to avoid the re-evaporation of the layer the thermal annealing in argon atmosphere with a pressure of 500 mbar was applied with the temperature of 550 °C. This process changes not only the grain size of CdS layer, but also the transmission at low wavelength regions (not shown here) with a slight improvement for the annealed case.

### **5.3.3 CdTe deposition and post-deposition treatment**

After CdS layers deposition and thermal annealing, CdTe was deposited using the standard process explained in chapter 3.

For this study, the typical CdTe layer thickness was 3.5 microns with quite compact morphology and grain size of about 1 micron. The CdTe morphology and the grain size are depending not only on

the substrate temperature during deposition, but also on the type of TCO. CdTe deposited on commercial ITO and on ITO+ZnO showed similar but not the same morphologies: grain size is typically around 1 micron wide but it results to be much more compact in the second case (see figure 5.1). Compared to the CSS deposited CdTe, the grains are quite small and they would need an activation treatment also to enlarge the grain sizes [9, 10].

## 5.4 Activation treatment

In our case we have applied two different processes in order to compare them and to analyze their effect on the evaporated CdTe layers: Freon and CdCl<sub>2</sub> activation treatments.

### 5.4.1 CdCl<sub>2</sub> treatment

The standard CdCl<sub>2</sub> treatment is applied by preparing a saturated solution of CdCl<sub>2</sub> in methanol.

Few drops are then put on the CdTe layer and the stacks are annealed in the air at a temperature ranging from 390 °C up to 430 °C for 30 minutes. The optimization of the device has brought to an optimum temperature of 410 °C.

### 5.4.2 Freon treatment

In this case the recrystallization treatment is made by a different method: an as-deposited cell is treated in a vacuum chamber at high temperature in the controlled mixture of chlorine containing gas Freon R-22, namely difluorochloromethane, and argon (with pressures from 10 up to 60 mbar for Freon and of 500 mbar for argon) for the period of between 5 and 25 minutes and at temperatures in the range of 400 °C to 450 °C [10]. At around 400 °C Freon dissociates, freeing chlorine, which is then reacting with CdTe forming CdCl<sub>2</sub>. The reaction between CdCl<sub>2</sub> and CdTe results in CdTe recrystallization and the CdTe grain boundaries passivation [11].

## 5.5 Morphological Analysis

The grain growth, recrystallization dynamics and the performance of the cells have been studied according to the different parameters of the recrystallization treatment: for example the ratio between Freon and argon in the mixture and the treatment temperature.

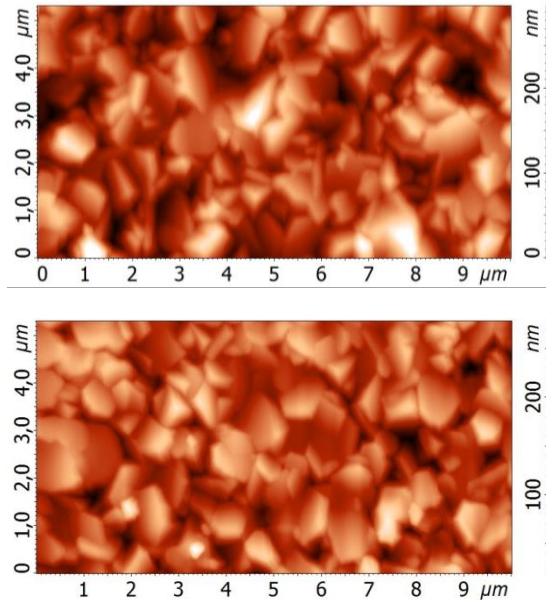


Figure 5.1: AFM pictures of as-deposited CdTe on CdS/commercial ITO stack (top) and on CdS/ZnO/ITO stack (bottom).

After deposition at 340 °C, CdTe is treated in Freon and argon ambient. Different partial pressures for Freon and different treatment temperatures have been applied. In figure 5.2 and figure 5.3 AFM images of the CdTe layers treated at temperatures from 400 to 440 °C are presented. The grain size is strictly dependent on the annealing temperature: most of the grains are around one micron wide for 400 °C, two microns for 420 °C and 5 microns for 440 °C.

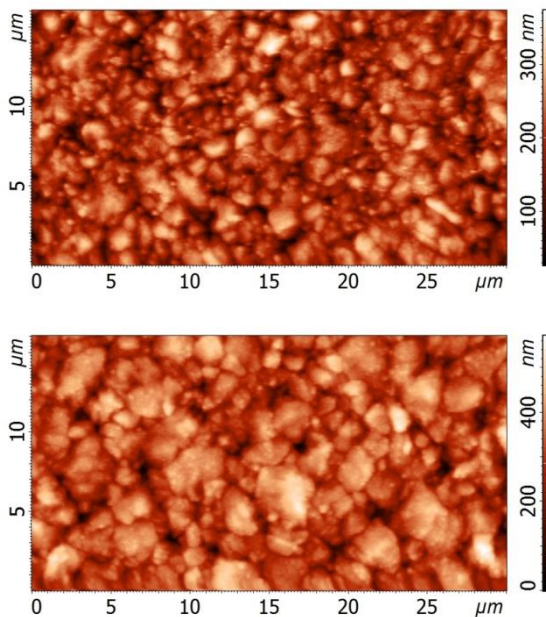


Figure 5.2: AFM images of CdTe treated with Freon and argon at 400 °C (top) and 420 °C (bottom).

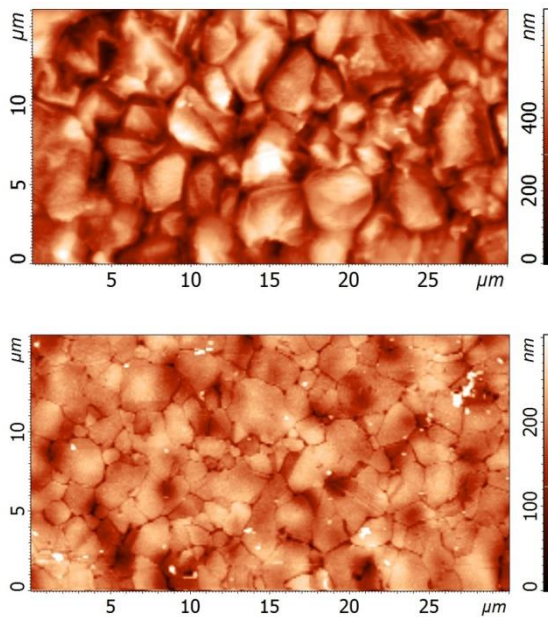


Figure 5.3: AFM images of CdTe treated with Freon and argon at 440 °C (top) and with CdCl<sub>2</sub> at 410 °C (bottom).

Higher temperatures were also applied but no significant increase of the grain size was registered.

However, if the Freon treatment assures good recrystallization of the grains,  $\text{CdCl}_2$  appears to deliver a much more compact morphology. It is also interesting to see that similar grain sizes are obtained for lower annealing temperatures (compare CdTe treated with  $\text{CdCl}_2$  at 410 °C in figure. 5.3 and CdTe treated with Freon and argon at 420° C in figure 5.2).

## 5.6 XRD Analysis

XRD measurements address different recrystallization processes of the CdTe layers depending on the TCO substrates and on the treatment temperature, as already suggested by AFM images.

In figure 5.4 (bottom) XRD pattern of as-deposited CdTe layer on CdS/commercial ITO is shown. CdTe crystals are strongly oriented as evidenced by the large diffraction intensity of the (111) peak in comparison with the intensities of the other reflections. This preferential orientation is typical for CdTe polycrystalline [7], but in our case it is clear only for the CdTe deposited on the CdS/commercial ITO substrates, while on the CdS/ZnO/ITO a lower degree of orientation in a different direction ((220) reflection) is observed (see figure 5.4 top).

As shown in figure 5.5, as a consequence of the activation treatment the recrystallization process of CdTe on commercial ITO takes place with different relative rate of growth of crystallite faces depending on the concentration of Freon in the gaseous atmosphere. In fact, after annealing the as-deposited CdTe crystallites change their orientation, which is different as a function of the chlorine concentration. When CdTe on CdS/commercial ITO is annealed in the presence of pure Freon the (111) peak reduces and (220) becomes the main one (see figure 5.5 top), whereas when a mixture of argon+Freon was employed (111), (220) and (422) are the main diffraction peaks (see figure 5.5 bottom).

When CdTe is deposited on CdS/ZnO/ITO, the orientations of the polycrystals are substantially different, even before the activation

treatment, as observed above. As a matter of fact the main reflection is the (220) line and no substantial change are detected for both  $\text{CdCl}_2$  and Freon treated layers. Only in the case when the samples are treated with  $\text{CdCl}_2$  at high temperature the crystals appear differently oriented (see increase of (311) reflection in figure 5.6 (bottom)).

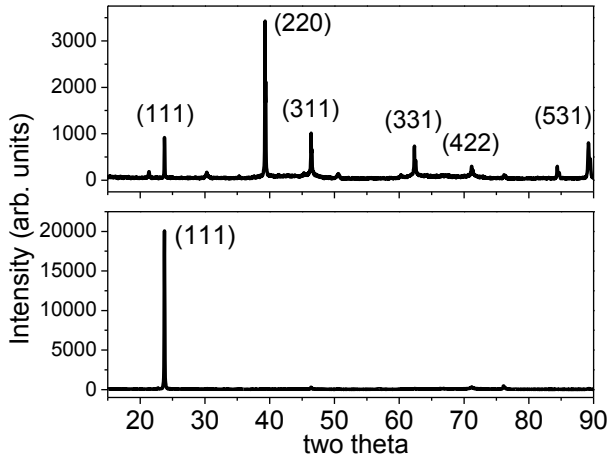


Figure 5.4: XRD spectra of as-deposited CdTe on CdS/ZnO/ITO (top) and on CdS/commercial ITO (bottom).

From these data, we observe that the nature and quality of the TCO substrate are not only essential in order to ensure a good efficiency of the devices but also strongly affect the growth of the CdTe crystallites.

Finally, the activation treatment of CdTe on CdS/commercial ITO performed at 420 °C with 50 mbar of Freon and no argon provides a device with the nature of the crystallites very similar to that ones present in the as-deposited CdTe/CdS/ITO/ZnO sample. In other words, due to the smaller effect of the activation treatment on the orientation of the grains, in the case of CdTe/CdS/ZnO/ITO prepared in our labs, we see this material as a more crystallized layer possessing higher quality than the CdTe on CdS/commercial ITO stacks.

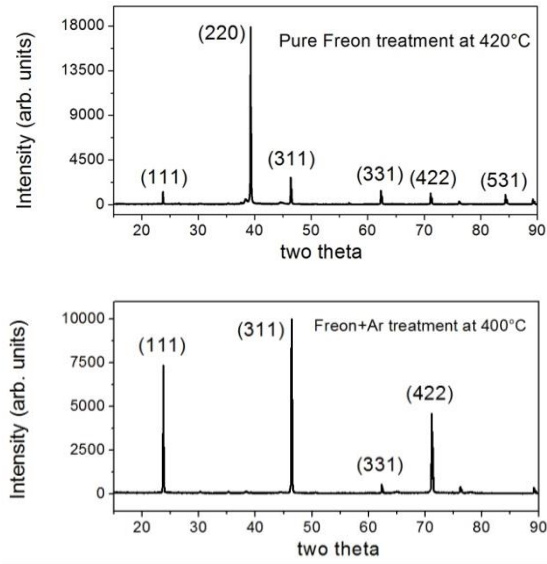


Figure 5.5: XRD spectra of recrystallized CdTe with Freon treatment in only Freon (top) and argon+Freon atmosphere (bottom) on CdS/commercial ITO.

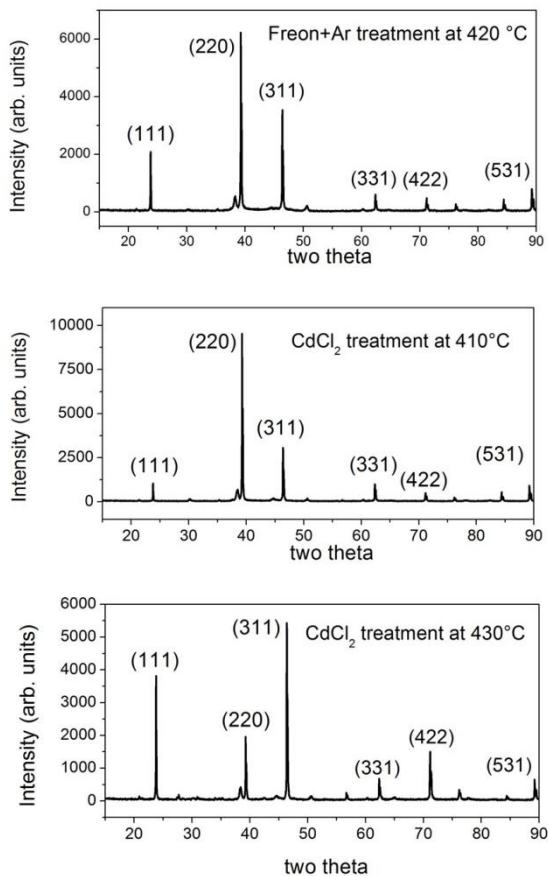


Figure 5.6: XRD spectra of the treated CdTe in argon+Freon atmosphere at 420 °C (top), with CdCl<sub>2</sub> at 410 °C (middle) and at 430 °C (bottom) on CdS/ZnO/ITO.

## 5.7 Back contact

Back contact is made by vacuum evaporation of Cu/Au stacks, as explained in chapter 1. Subsequently the air annealing of the back contact is applied at 200 °C in air for 20 minutes in order to diffuse Cu in CdTe and make an ohmic contact [12].

In case of Freon treatment, the treated CdTe is not etched since the surface is free of CdCl<sub>2</sub> (re-evaporated at high temperature in vacuum) and a tellurium rich layer is made during the activation process [11].

In case of CdCl<sub>2</sub> treatment, a Br-MeOH etching is applied in order to remove the CdCl<sub>2</sub> layer and to prepare the surface for the Cu/Au deposition. However the removal of the CdCl<sub>2</sub> in case of wet treatment is quite difficult [8].

The deposition of copper results to be very important, a higher amount of copper improves the back contact but at the same time reduces the shunt resistance resulting in a lower fill factor.

Moreover, the required copper amount is also dependent on the different CdTe treated layer. We have registered for Freon treated CdTe devices four times the amount of copper is needed for a reasonable efficiency compared to the CdCl<sub>2</sub> treated cells. This is consistent with the fact that activation by Freon is much weaker than the one performed with CdCl<sub>2</sub> as reported above. On the other hand using a lower amount of copper allows achieving a better working cell and consequently a higher efficiency, as shown in the next part of this chapter.

## 5.8 Performance

A large amount of different devices has been made, by optimizing both CdCl<sub>2</sub> and Freon treatment for CdTe deposited on the different stacks described before.

The highest performance was given by CdCl<sub>2</sub> treated cells and with stronger CdS/TCO stacks. This means that the most performing TCO was the one made with high temperature deposited ZnO/ITO with enhanced ability and prevention of sodium and indium diffusion

and with thicker CdS or CdS annealed at high temperature. Moreover, only two nm of copper with 50 nm of gold are necessary for a good contact. With this configuration efficiencies exceeding 10 % are routinely obtained.

If Freon treatment is applied, much lower efficiencies are registered; highest efficiencies are obtained with 8 nm of copper. However, much lower shunt resistance gives lower fill factor and lower open circuit voltage.

If a 2 nm copper contact is applied on a Freon treated cell a very low efficiency is performed (see figure 5.7). Anyway with more aggressive Freon treatment (by higher Freon partial pressures or higher temperature) bigger grain size is obtained but not higher efficiencies, excess of Freon pressure have resulted in shunted device.

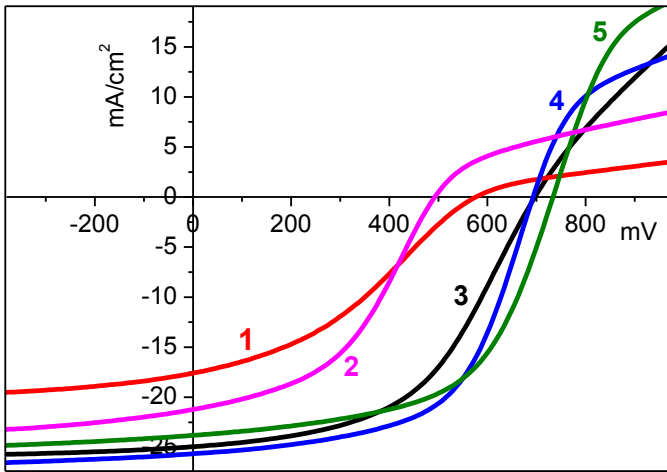


Figure 5.7: J-V measurement of solar cells with 1) CdTe treated with only Freon; 2) Freon treated CdTe with 2 nm of Cu; 3) Freon treated CdTe with 8 nm of Cu; 4) CdCl<sub>2</sub> treated CdTe with CdS annealed in argon; 5) CdCl<sub>2</sub> treated CdTe with CdS annealed in vacuum.

In figure 5.7 the J-V curves of our best cells, treated with CdCl<sub>2</sub> and Freon, are presented and their respective performance values are shown in Table 5.1.

The cells made with  $\text{CdCl}_2$  treatment exhibit efficiencies from 10 to 11 %, with current density in the range of 22 to 25  $\text{mA/cm}^2$ ,  $V_{oc}$  exceeding 700 mV and FF from 55 to 60 %. The relatively low  $V_{oc}$  and FF are connected with relatively low  $R_{sh}$ . This can be explained by an excessive consumption of CdS into the CdTe layer.

The best results were obtained with thicker CdS (more than 500 nm) annealed in vacuum at 450 °C (see curve 5 in figure 5.7) or with 250 nm CdS annealed at 550 °C in argon atmosphere (see curve 4 in figure 5.7) to prevent re-evaporation.

Roll over in  $\text{CdCl}_2$  treated cells can be connected with the treatment method. As a matter of fact, wet  $\text{CdCl}_2$  treatment gives place to a thin cadmium oxide layer, which is difficult to remove with Br-MeOH etching [8].

Freon-treated cells show lower efficiencies than  $\text{CdCl}_2$  treated ones. The highest achieved efficiency for this treatment is 8.7 % (see curve 3 in figure 5.7). Although the Freon treated cells would not need a post deposition etching [11], a good ohmic back contact was not easily reproducible. Many of our Freon-treated cells have shown a roll-over effect on the positive part of the curve (figure 8 cells 1 and 2).

Table 5.1: Best cells performance.

N	Treatment type	$V_{oc}$ mV	$J_{sc}$ $\text{mA/cm}^2$	FF %	$\eta$ %	Cu nm
1	Freon	578	17.6	35.3	3.6	8
2	Ar+Freon	493	21.2	44.8	4.7	2
3	Ar+Freon	697	24.9	50.2	8.7	8
4	$\text{CdCl}_2$	697	25.6	57.7	10.3	2
5	$\text{CdCl}_2$	740	23.8	56.7	10	2

## 5.9 Conclusions

Thin film solar cells were made with a low substrate temperature deposition process. Annealing of CdS layer in argon atmosphere at 550 °C resulted in bigger grain size and in a slight improvement of

the film transmission at low wavelength regions comparing with CdS annealed in vacuum at 450 °C. More compact CdTe was obtained on ITO+ZnO stacks. The XRD measurements revealed that the pure Freon activation treatment (without argon) of the CdTe on CdS/commercial ITO gives rise to a crystallized layer very similar to that one present in the as-deposited CdTe on CdS/ZnO/ITO. For this reason, the latter can be considered as more crystallized and therefore, in terms of quality, it is better than the former.

CdTe deposited on CdS/commercial ITO stacks lost preferred orientation during both CdCl<sub>2</sub> and Freon treatments. CdTe deposited on CdS/ZnO/ITO stacks kept the (220) preferential orientation for both CdCl<sub>2</sub> and Freon treated layers and only in case of high temperature CdCl<sub>2</sub> treatment the crystals were more randomly oriented. This can be explained by higher stability and better crystalline quality of CdTe films deposited on ITO+ZnO stacks.

In case of Freon treated CdTe, four times more amount of copper was needed for a reasonable efficiency compared to the CdCl<sub>2</sub> treated cells. This can be explained with a lower ability of Freon treatment to activate the absorber layer. Solar cells with CdCl<sub>2</sub> treated CdTe had higher efficiency then with Freon treated CdTe.

## 5.10 References

- [1] N. Romeo, A. Bosio, A. Romeo, S. Mazzamuto and V. Canevari, 21st EU PVSEC, 2006, pages 1857-1860.
- [2] A. Salavei, I. Rimmaudo, F. Piccinelli, V. Allodi, A. Romeo, A. Bosio, N. Romeo, S. Mazzamuto, D. Menossi, Proceedings of the 26th European Photovoltaic Solar Energy Conference, 2011.
- [3] A. Salavei, I. Rimmaudo, F. Piccinelli, P. Zabierowski and A. Romeo, Solar Energy Materials & Solar Cells 112 (2013) 190–195.
- [4] R. Bube, Photovoltaic materials, 1998, Imperial College Press.
- [5] X. Wu, Solar Energy 77 (2004) 803–814.

- [6] A. Gupta, V. Parikh, A. D. Compaan, *Solar Energy Materials & Solar Cells* 90 (2006) 2263–2271.
- [7] A. Romeo, D.L. Bätzner, H. Zogg, A.N. Tiwari. *Thin Solid Films*, Volume 361-362 (2000) Pages 420-425.
- [8] D.M. Waters, D. Niles, T.A. Gessert, D. Albin, D.H. Rose, and P. Sheldon, 1998, NREL/CP-530-23876.
- [9] A. Romeo, M. Terheggen, D. Abou-Ras, D.L.Bätzner, F.-J. Haug, M. Kälin, D. Rudmann, A.N. Tiwari. *Progress in Photovoltaics: Research and Applications*, Volume 12, Issue 2-3, 2004, pp 93-111.
- [10] A. Romeo, G. Khrypunov, S. Galassini, H. Zogg and A.N. Tiwari, N.Romeo, A.Bosio, S. Mazzamuto. *Proceedings of 22nd European Photovoltaic Solar Energy Conference*, 2007, pp 2367-2372.
- [11] A. Romeo, S. Buecheler, M. Giarola, G.Mariotto and A.N. Tiwari, N.Romeo , A.Bosio , S. Mazzamuto. *Thin Solid Films*, Volume 517, Issue 7, 2 February 2009, Pages 2132-2135.
- [12] T.D. Dzhafarov, S.S. Yesilkaya, N. Yilmaz Canli and M. Caliskan. *Solar Energy Materials and Solar Cells*, Volume 85, issue 3, 2005, 371-383.

# **6 Influence of CdTe thickness on structural and electrical properties of CdTe/CdS solar cells**

## **6.1 Abstract**

The influence of CdTe thickness on structural and electrical properties of CdTe/CdS solar cells was studied. Solar cells with CdTe thicknesses of 0.7, 1 and 1.8 microns were fabricated. Structural properties of these thin absorbers and performances of respective solar cells were studied and compared with standard ones. Dependence of CdTe grains size from the layer thickness was observed for both as-deposited and treated cases. Recrystallization, loss of preferential orientation and increase of grains size after activation treatment were observed for all the layers. X-ray diffraction measurements showed presence of  $\text{CdS}_x\text{Te}_{1-x}$  intermixed layer in 0.7  $\mu\text{m}$  thick CdTe absorber after the activation treatment. To confirm this, lattice parameter and the energy band gap of thin absorbers were calculated. According to these values  $\text{CdS}_x\text{Te}_{1-x}$  intermixed layer is a significant part of the absorber layers in solar cells with CdTe thickness less than 1  $\mu\text{m}$ . Solar cells showed a different electrical behaviour in terms of open circuit voltage and fill factor. Efficiencies range from 7 % for 0.7  $\mu\text{m}$  thin CdTe cells up to 13.5 % for standard thickness.

Parts of this chapter are published in the references [1, 2].

## 6.2 Introduction

A large-scale CdTe PV module production in the order of terawatts could be limited by tellurium scarcity as this is a rare element and generally mined as by-product, but reducing the CdTe thickness down to 1.5 microns would solve this issue. [3]. Moreover, reducing the absorber thickness would result in a relevant reduction of the production costs. There are, however, issues to be considered, such as formation of pinholes, lower crystallization, and different possible effects on materials diffusion within the interfaces.

CdTe solar cells are typically produced with thicknesses between 4 and 6 microns [4]. This assures good coverage avoiding pin-holes and delivering high open circuit voltage devices. On the other hand, because of the high absorption coefficient, two microns are enough for absorbing all the light and converting sunlight into electricity [5], but in this case device performance is lower and the structural and electrical properties of thin absorbers are different [6].

This chapter presents the study of CdTe solar cells fabricated by vacuum evaporation with different CdTe thicknesses. Several cells with absorber thickness from 0.7 up to 6 microns have been fabricated by using a specific optimized deposition process. The study of physical properties of CdTe absorbers with different thicknesses and performance study of the devices made without changing the other layers is presented.

## 6.3 Experimental details

CdTe solar cells were prepared using vacuum evaporation. The standard device was made with 400 nm CdS and 6000 nm CdTe. In our process the CdCl<sub>2</sub> treatment is made by depositing drops of CdCl<sub>2</sub> powder saturated in methanol followed by heating in air at 410 °C. The amount of CdCl<sub>2</sub> is modulated by measuring the amount of the solution. The cells are then finished with a standard copper/gold back contact with 2 nm Cu and 50 nm Au, deposited by vacuum evaporation. The back contact is annealed at 190 °C in air

for 20 minutes. Typical efficiencies range from 11 to 13 % according to the preparation procedure.

For this specific work, cells with different absorber thicknesses were prepared. Single CdTe layers were analyzed, including their physical properties and the growth on CdS. Thicknesses of 0.7, 1, 1.8, 4, and 6 microns were evaluated. CdCl<sub>2</sub> treatment was modulated to the amount of CdTe thickness, by reducing it for thinner CdTe. A comparison of the thin absorbers transformed with the same activation treatment has also been provided.

## 6.4 Results and Discussion

### 6.4.1 Morphology of CdTe

As-deposited and treated CdTe layers were observed with a NT-MDT Solver Pro AFM in semi-contact mode. A different CdTe grain sizes on the CdS/ZnO/ITO stacks were observed for different CdTe thicknesses. As expected, by increasing the layer thickness, grains increase and the difference becomes very large, especially for the as-deposited case where the morphology depends only on growth conditions.

In figure 6.1 grain sizes of 1.8 and 6 microns thick CdTe on the CdS/ZnO/ITO stacks are compared. For thin absorber a homogeneous morphology with similar grains in the whole layer was observed. This changed drastically for 6 microns CdTe, where sizes have higher order of magnitudes but, at the same time, showed a wide range of small and big grains. However, while in the thin CdTe the recrystallization brought an overall increase in the grain size of up to one order of magnitude, in the thick CdTe this enlargement is only from two to three times the initial size. An evident change in morphology with more compact grains was also registered for both cases.

Morphology and grain size has been addressed for all the different thicknesses by analyzing the AFM images and extracting the average size and mean quadratic deviation of as-deposited CdTe layers by Image Analysis 3.5 (NT-MDT), as shown in figure 6.2.

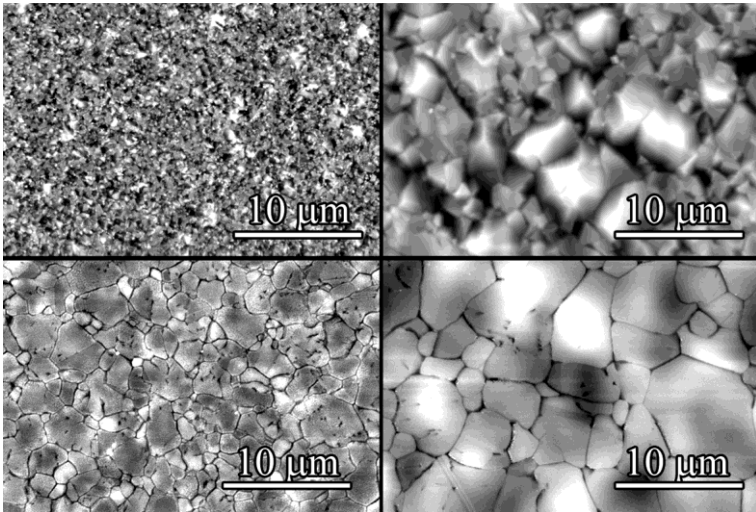


Figure: 6.1: AFM images of 1.8 and 6  $\mu\text{m}$  as-deposited CdTe (top) and of 1.8 and 6  $\mu\text{m}$  treated CdTe (bottom).

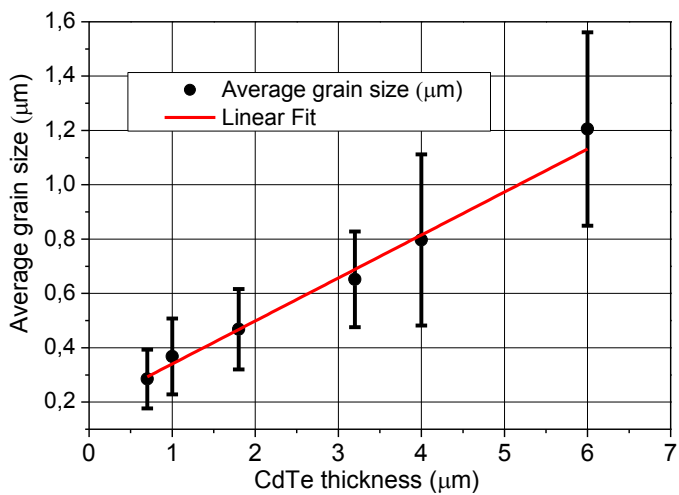


Figure 6.2: Average grain size versus thickness, measured from AFM images with relative mean quadratic deviation.

It is clearly evident that there is a linear dependence of grain size with thickness (as also observed by Durose et al. [7]). Most interesting, there is a constant increase in grain size spreading: so that for thick CdTe layers, grains range from 0.5 to 5 microns (see figure 6.1).

The difference in grain size with thickness is still maintained after CdCl<sub>2</sub> treatment, despite a general increase from the as-deposited case, but the morphology is more compact and grains are more similar to each other.

#### 6.4.2 X-ray diffraction of CdTe layers

CdTe layers with 0.7, 1, 1.8 and 6 microns thickness deposited on CdS/ZnO/ITO stacks were analyzed in both as-deposited and treated cases by XRD. In the as-deposited case the layers show a very similar crystallization. The crystallites are highly oriented along the (111) direction with no other peaks observed, irrespective of the absorber thickness. This indicates that the grains grow with the same orientation, which is also suggested by the AFM images wherein similar morphologies with different grain sizes can be seen.

On the other hand, the structure becomes very much different after the application of CdCl<sub>2</sub> treatment (see figure 6.3). The grain orientation is clearly depending on the different CdTe thickness, where the thinner CdTe still keeps a relative (111) preferred orientation which tends to be reduced by the increase of the thickness, so that the 6 microns thick CdTe has changed its preferred orientation to (311). So it is observed that a highly randomized CdTe, generally reported in literature [4], is actually seen for thicker CdTe.

Moreover for 0.7 and 1 microns treated CdTe, some clear CdS peaks are observed. Considering that x-rays are able to penetrate the layer down to one micron from the surface, this states that in this case the CdS-CdTe intermixed layer is a consistent part of the device. This is even more outlined in the thinner absorber where a peak attributed to an intermixed layer [(Cd<sub>5</sub>S<sub>4</sub>Te)<sub>0.8</sub>] is observed (see figure 6.3), suggesting that in the very thin case the intermixed CdS<sub>1-x</sub>Te<sub>x</sub> layer is not far from the back contact and it occupies a relevant part of the absorber.

In order to further investigate this aspect we analyzed the XRD peaks by applying a calculation, which was firstly introduced by Nelson [8] and Taylor [9] and subsequently applied by Moutinho et al. [10]. For cubic structure it is possible to calculate the lattice parameter just by analyzing the positions of the XRD peaks with a very high precision.

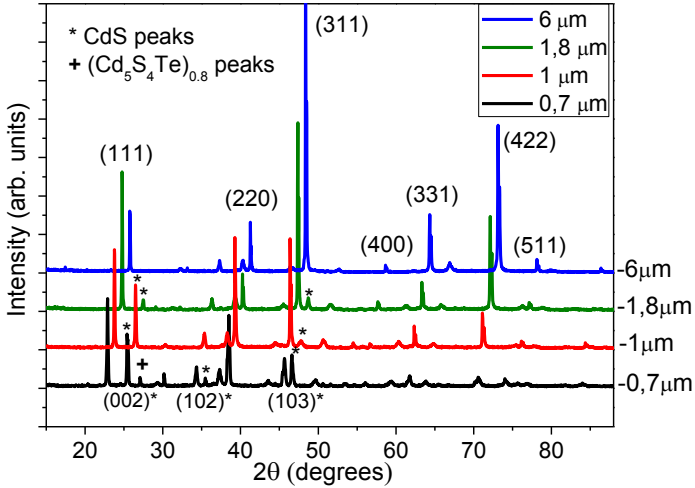


Figure 6.3: XRD patterns of the treated CdTe absorbers with different thicknesses.

Lattice parameters of treated CdTe with different thicknesses have been calculated by fitting the position of the different peaks as shown in figure 6.4, where the upper and lower limits of the thickness range are reported. The 0.7  $\mu\text{m}$  treated CdTe shows a very small lattice parameter (6.451  $\text{\AA}$ ) in respect to the standard 6  $\mu\text{m}$  one (6.487  $\text{\AA}$ ) and much smaller than the standard lattice parameter referred to the powder (6.481  $\text{\AA}$ ) [10]. As generally known, intermixing of CdTe with sulphur brings to a reduction of lattice parameter as well as of band gap. This is supporting the fact suggested by the XRD patterns that the very thin absorber is made of an intermixed layer of CdTe and CdS.

To have an additional indication of these phenomena, transmission spectra of the different absorbers were collected and the corresponding band gaps have been extracted following the well-known Tauc relation for direct transitions [11]:

$$\alpha hv = C(hv - E_g^d)^{1/2} \quad (6.1)$$

Where in the graph  $(\alpha hv)^2$  vs  $hv$  the intercept is the band gap that we want to calculate (see figure 6.5). The calculations were processed with very precise fittings. This method is approximate for direct electronic band-to-band transitions because it assumes that the refractive index is constant in the energy range considered. Thus, the calculated band gap may be only taken as a rough estimate.

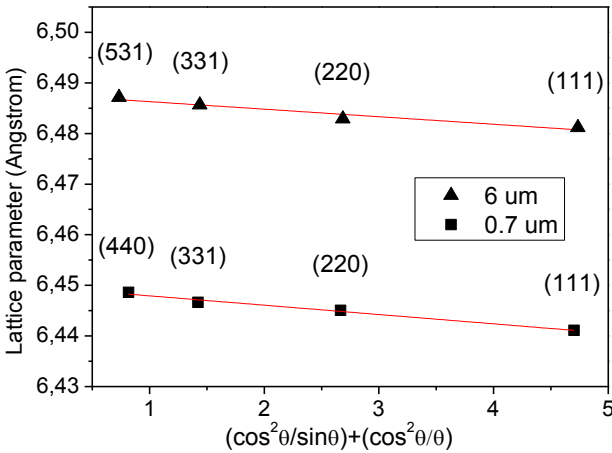


Figure 6.4: Lattice parameters of 0.7  $\mu\text{m}$  and 6  $\mu\text{m}$  CdTe after  $\text{CdCl}_2$  treatment.

In table 6.1, band gaps and lattice parameters of the various samples are presented. The different absorbers have a similar band gap before treatment suggesting that there is not a strong difference in the growth conditions in relation to the CdTe thickness as also

seen in the XRD patterns, however, when the activation treatment is applied, we observe a general reduction of the band gap. This effect is particularly strong for the thinner absorber confirming a strong intermixing of the CdS and CdTe in the whole layer as also suggested by the lattice parameter calculation.

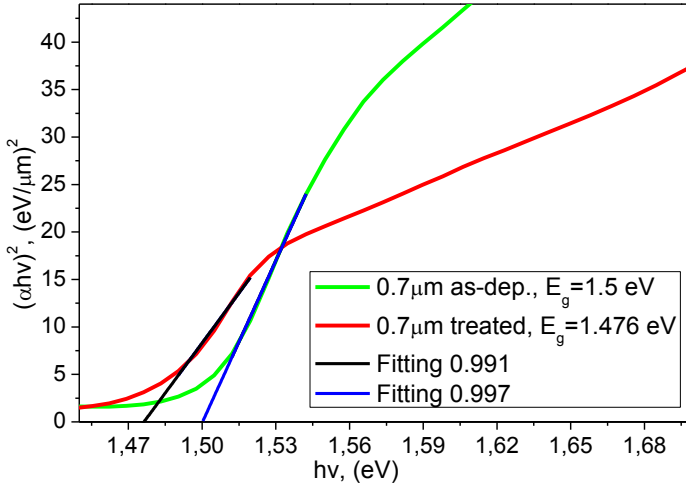


Figure 6.5: The dependence of  $(\alpha hv)$  on photon energy for 0.7  $\mu\text{m}$  thick as-deposited and treated CdTe layers, from which the optical band gap is determined.

For thicker absorbers a significant difference between activated and not activated samples is not observed: their lattice parameters in the as-deposited case are similar to the ones of the recrystallized thinner samples and lower than the ones of as-deposited thinner samples.

In general, the high lattice parameter is attributed to compressive stress in the in-plane parallel to the substrate surface due to lattice mismatch and difference in thermal expansion coefficients between the CdTe and the CdS films [10]. This stress is clearly reduced when CdTe thickness is increasing and the bulk CdTe is far away from the

junction. For this reason the polycrystals are in a more stable condition and the post-treatment structure changes are minimized.

Table 6.1: Lattice parameters and band gaps of as-deposited and treated CdTe with different thicknesses, values uncertainties are on the last decimal digit.

Thickness (microns)	Activation treatment	Lattice parameter ( $\text{\AA}$ )	Band gap (eV)
0.7	treated	6.451	1.48
0.7	As-dep	6.494	1.50
1	treated	6.488	1.49
1	As-dep	6.498	1.50
1.8	treated	6.487	1.50
1.8	As-dep	6.484	1.50
6	treated	6.487	1.50
6	As-dep	6.485	1.50

## 6.5 Solar cell devices

Several different devices have been prepared with the above-mentioned CdTe thicknesses. A rough optimization procedure has been made, assuming that with less CdTe a reduced CdCl<sub>2</sub> amount was necessary to avoid over-treatment, which results in excessive diffusion of CdS into CdTe [12].

Our CdTe deposition system, based on vacuum evaporation, allows to have a very fine control of the absorber growth and to reduce formation of pin-holes. For this reason we have obtained very promising efficiencies even for ultra-thin absorbers, despite the performance is anyway limited compared to the 6 microns case, as shown in figure 6.6.

From the value of fill factor, it is interesting to observe that with just 1 micron CdTe we have almost no shunts and the stronger limitation comes particularly from the low current density, which is increasing with the thickness increase. In the ultra thin case instead,

higher  $J_{sc}$  and lower  $V_{oc}$  are registered, partly due to shunts but also surely attributable to the presence of the strongly intermixed bulk with lower band gap reported above. This device is obtained with a reduced amount of  $CdCl_2$  of 180  $\mu l$  instead of the typical 720  $\mu l$ , suggesting that the excessive intermixing is not due to a higher  $CdCl_2$  vs  $CdTe$  ratio but to a reduced thickness where the junction is very near to the back contact. A confirmation of this condition is given by the behaviour of the J-V characteristics of ultra-thin layers with the different amount of copper and post-deposition annealing. It has been observed that for these samples no annealing after copper deposition was necessary to get rid of the roll-over in the first quadrant of the I-V curves, which demonstrates that even with lower mobility, the path for ultra thin layers is so reduced that there is no need to improve the carrier concentration as also observed by Hädrich et al. [13].

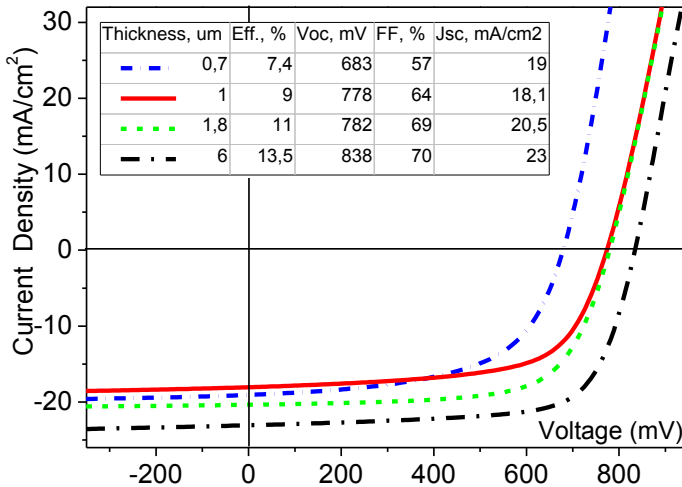


Figure 6.6: J-V characteristics of solar cells made with different CdTe thicknesses.

For comparison a set of devices with different CdTe thickness but with same  $CdCl_2$  amount has been made. This shows that even with the same amount of solution prepared for the 6 microns case,

cells with 0.7 microns thick CdTe have very similar performance (around 7 %) to the ones made with only 180  $\mu\text{l}$ . Again this indicates that the reduction in efficiency is mostly due to a different solar cell structure as described a few lines before.

The lower efficiency of the 0.7  $\mu\text{m}$  CdTe devices can be attributed to the fact that a large part of the absorber is an intermixed compound of  $\text{CdS}_x\text{Te}_{1-x}$ , as attested by energy band gap, lattice parameter extraction and especially by the detection of the  $(\text{Cd}_5\text{S}_4\text{Te})_{0.8}$  XRD peak. As a matter of fact a band gap of intermixed absorber delivers lower open circuit voltage and higher current as effectively observed from the J-V measurements.

The slightly lower efficiencies of solar cells with 1 and 1.8  $\mu\text{m}$  CdTe compared to the standard one are given particularly by low current density. Admittance spectroscopy and drive level capacitance measurements [2] reveal that the main reason is due to the extension of the depletion region to the back contact even at high temperatures as also suggested by Beach et al. [14].

## 6.6 Conclusions

Solar cells with different absorber layer thickness (0.7  $\mu\text{m}$ , 1  $\mu\text{m}$  and 1.8  $\mu\text{m}$ ) were prepared and compared with the standard 6  $\mu\text{m}$  thick CdTe ones.

Despite the main scope of this study was exclusively to identify the different structural and electrical properties of devices with thin CdTe, solar cells with absorber layer of 0.7  $\mu\text{m}$  have demonstrated a promising efficiency exceeding 7 %. For cells with absorber thickness of 1  $\mu\text{m}$  and of 1.8  $\mu\text{m}$  the efficiencies were respectively 9 % and 11 %, anyway lower than the one of our standard devices with efficiencies around 13.5 %.

A linear increase of CdTe grain size with the increasing of CdTe thickness was observed. On the other hand for as-deposited absorber layers with different thicknesses no significant difference was found in calculated lattice parameter and band gap energy. Moreover they all showed a strong (111) preferential orientation in the XRD patterns.

After  $\text{CdCl}_2$  treatment the CdTe grain size increases but still maintaining a similar difference between each other. The (111) preferred orientation is lost only for the thicker absorbers and lattice parameter is relaxed for thinner ones.

After a first comparison of devices made with the same fabrication parameters,  $\text{CdCl}_2$  treatment, back contact deposition and annealing steps were adjusted for different absorber thicknesses in order to optimize their performance. However no significant change in performance between devices with standard (720  $\mu\text{l}$ ) and reduced amount (180  $\mu\text{l}$ ) of  $\text{CdCl}_2$  has been registered. On the contrary, a small amount of copper (even without post deposition annealing) is enough for thin absorbers to collect the carriers.

Most important, we could observe that lower efficiencies for the thinnest absorber can be attributed to the intermixed compound of  $\text{CdS}_x\text{Te}_{1-x}$  as absorber, while for solar cells with 1 and 1.8  $\mu\text{m}$  CdTe lower efficiencies are connected to the low current density due to the extension of depletion region to the back contact.

## 6.7 References

- [1] A. Salavei, I. Rimmaudo, F. Piccinelli, A. Romeo, Thin solid films, In Press, Corrected Proof, Available online 16 December 2012.
- [2] I.Rimmaudo, A. Salavei, F. Piccinelli, D. Menossi, N. Romeo, A. Romeo, Proceedings of the 27th European Photovoltaic Solar Energy Conference, 2012.
- [3] V. Fthenakis, Renewable and Sustainable Energy Reviews. 13 (2009) 2746–2750.
- [4] A. Romeo, M. Terheggen, D. Abou-Ras, D. L. Batzner, F.-J. Haug, M. Kalin, D. Rudmann and A. N. Tiwari, Prog. Photovolt: Res. Appl. 12 (2004) 93-111.
- [5] A.L. Fahrenbruch, R.H. Bube, Fundamentals of Solar Cells, Academic Press, New-York NY1983, p.332.

- [6] A. Bosio, N. Romeo, S. Mazzamuto, V. Canevari, *Progress in Crystal Growth and Characterization of Materials*, 2 (2006) 247-279.
- [7] K. Durose, M.A. Cousins, D.S. Boyle, J. Beier, D. Bonnet, *Thin Solid Films* 403-404 (2002) 396-404.
- [8] J.B. Nelson and D.P. Riley, *Proc. Phys. Soc.* 57 (The Physical Society, London, 1945) p. 160.
- [9] A. Taylor and H. Sinclair, *Proc. Phys. Soc.* 57 (The Physical Society, London, 1945) p. 126.
- [10] H.R. Moutinho, M.M. Al-Jassim, F.A. Abufoltuh, D.H. Levi, P.C. Dippo, R.G. Dhere, and L.L. Kazmerski, 26th IEEE Photovoltaic Specialists Conference, 1, 30 (1997) 3.
- [11] J. Tauc, *Amorphous and Liquid Semiconductors*, Plenum press, 1974, p.175.
- [12] I. Rimmaudo, A. Salavei, A. Romeo, *Thin solid films*, In Press, Corrected Proof, Available online 16 December 2012.
- [13] M. Hadrich, C. Heisler, U. Reislohnner, C.Kraft, H. Metzner, *Thin Solid Films* 519 (2011) 7156-7159.
- [14] J. Beach, F-H Seymour, V.I. Kaydanov and T.R. Ohno, NREL Report 520-41097.

## **7 Flexible CdTe solar cells by a low temperature process on ITO/ZnO coated polymers**

### **7.1 Abstract**

Thin film CdS/CdTe solar cells were grown on flexible substrates with low substrate temperature deposition process and compared with solar cells grown on glass. Our standard process (see chapter 3) was optimized in order to allow the use of flexible substrates. Activation treatment was the most challenging step in fabrication process. The flexible nature of the substrate resulted in inhomogeneity and low reproducibility of the treatment. Atomic force microscopy and X-ray diffraction analysis showed that there are no significant structural and morphological differences between layers grown on flexible and rigid substrates. Solar cells on flexible substrates were less efficient than solar cells on glass because of much lower current values. The main reason for low current is the limited transparency of flexible substrates, which results in absorption losses. Our best flexible solar cell showed efficiency of 10 %. Laser scribing tests on the different stacks deposited on the flexible substrates by fiber lasers were made.

This chapter is based on the publication [1] presented at the 27<sup>th</sup> European Photovoltaic Solar Energy Conference in Frankfurt.

## 7.2 Introduction

As mentioned in previous chapters, low production energy, low amount of needed materials, low price and high scalability are advantages of thin film CdS/CdTe solar cells [2, 3]. But another very important advantage of these technologies is that since they are extremely thin devices, if deposited on flexible substrates they also become flexible.

Thin film solar cells deposited on a flexible substrate are easier to integrate in buildings; they also have a very high specific power for consumer electronics and space applications [4]. Cells of equivalent performance can have specific power (kW/kg) 500 times bigger on 12.5  $\mu\text{m}$  polyimide as compared to 3 mm glass substrates [5].

Flexible CdTe solar cells have shown efficiencies comparable but still lower than cells made on glass [6]. There are two reasons for efficiency loss: current density loss due to the lower polymer transparency and lack of rigidity which does not enable easy handling, giving place to possible pin-holes and cracks in the deposited films.

As far as polymer stability is crucially depending on temperature only low temperature fabrication processes are suitable for the production of solar cells on polymers. Vasko et al. and Drayton et al. from the University of Toledo have presented a sputtering process for fabrication of CdTe cells on polyimide with efficiencies of 10.5% [5, 7]. A record efficiency of 13.8% for flexible CdTe solar cells in superstrate configuration has been achieved by the group of A. N. Tiwari (EMPA laboratories, Switzerland) with a polyimide substrate by using vacuum evaporation and vacuum deposition of  $\text{CdCl}_2$  [8]. In all mentioned cases ZnO doped with Al was used as a front contact.

In this chapter we show a CdTe solar cell fabrication process in superstrate configuration on flexible polyimides with an ITO/ZnO front contact and wet  $\text{CdCl}_2$  treatment. Optimization of fabrication process and technological aspects of the device were taken into account. Results are compared to our standard process on glass.

The choice for indium tin oxide as a front contact has been taken because of its high conductivity and better stability compared to ZnO doped with Al [9, 10 and 11]. An intrinsic zinc oxide buffer layer is applied to avoid indium diffusion and to increase the open-circuit voltage.

### 7.3 Experimental details

To develop a fabrication method for flexible CdTe devices, we use our standard process (see chapter 3). The solar cells were first optimized on glass by engineering a deposition process with a substrate temperature that should not exceed 450 °C in order to prevent degradation of the polymer.

A specific study to find a suitable polymer that could withstand a high temperature and provide sufficient transparency was made. Comparison of the transparency of different polymers after the thermal annealing, which is required during fabrication process, provided in air at 450 °C for 30 min (compare transparency of UPILEX and Kaneka on fig 7.1) showed that UPILEX polymers are most suitable substrates for fabrication process. A similar polymer has already been used in the past and was shown to be the best choice [4]. During the process polyimide films were attached to glass in order to avoid bending.

The front contact was made by depositing 550 nm of ITO by direct current magnetron sputtering on the substrate, subsequently 120 nm of ZnO were deposited by reactive radio frequency magnetron sputtering on top of the ITO layer. Substrate temperature during deposition was 100 °C, lower than the typical value for the glass substrate (300 °C).

Moreover, the deposition step of CdS window layer has been changed. The temperature of thermal annealing was reduced from 450 °C down to 430 °C in order to prevent degradation of polymers substrates. Then CdS and CdTe were deposited at our standard conditions. Wet CdCl<sub>2</sub> treatment was used for cells activation. It is important to mention that the wet treatment step acts out the major difficulties. Deviation of the polymer flatness can result in

unhomogeneity and therefore in irreproducibility of the treatment. For this reason a more concentrated solution of  $\text{CdCl}_2$  in methanol was applied; providing more reproducible results. Finally the standard back contact was made to the samples.

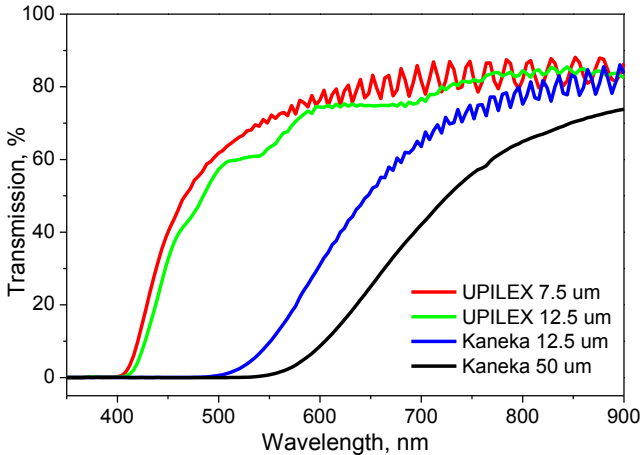


Figure 7.1: Transmission spectra of different polymers after thermal annealing at 450 °C in air for 30 minutes.

## 7.4 Results and discussion

### 7.4.1 Layer and Device Characterization

Analysis of treated CdTe films with AFM showed that the morphology of the layers made on glass and polyimide is very similar. Grain size of treated CdTe layers on glass is slightly bigger than on polyimides (see figure 7.2). The grains of CdTe on CdS/TCO/polyimide are in range of 1 to 8 microns, while some grains of CdTe on CdS/TCO/glass reach size of 10 microns. One possible reason for it is the lower annealing temperature of CdS. CdS deposited on polyimide was annealed at 430 °C while CdS deposited on glass was annealed at 450 °C. Nevertheless, wet  $\text{CdCl}_2$  treatment applied on CdTe films deposited on polyimide/ITO/ZnO/CdS results

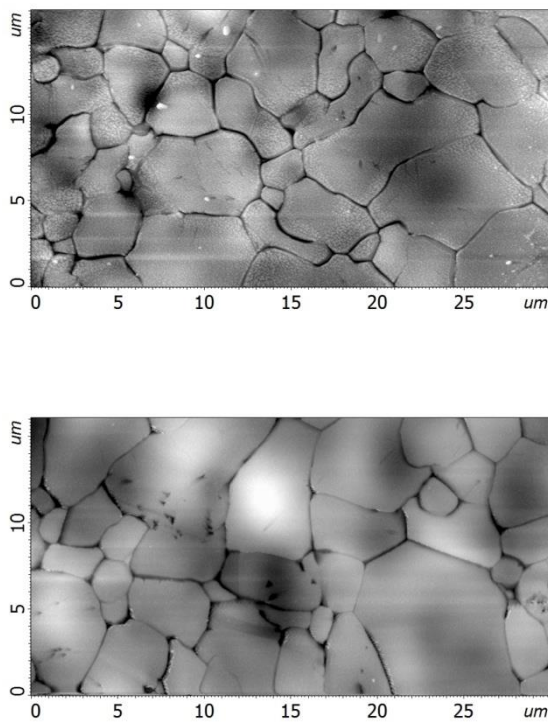


Figure 7.2: AFM pictures of treated CdTe on polyimide (top) and on glass (bottom).

in the typical increase of grain size with a compact morphology [12]. We can conclude that changing the substrate from glass to polyimide does not affect the CdTe morphology.

CdTe layers deposited on glass/ITO/ZnO/CdS and polyimide/ITO/ZnO/CdS stacks have been analyzed by X-ray diffraction in both as-deposited and treated cases.

Figure 7.3 shows XRD patterns of as-deposited CdTe layers on polyimide/ITO/ZnO/CdS and glass/ITO/ZnO/CdS stacks. As-deposited CdTe layers have a strong (111) preferred orientation in both cases. This is a typical behaviour of CdTe grown on glass substrates [12] and this demonstrates that CdTe grows with the same preferential orientation on polyimide as on glass. At the same time CdTe layers deposited on polyimide/ITO/ZnO/CdS stacks have more randomized structure (compare intensities of (220), (311) and (422) peaks on figure 7.3). The different behaviour could be partly explained by the lower temperature of CdS annealing, giving a different structure to CdS polycrystals and, consequently, also to the CdTe deposited on it. Another possible reason could come from the effect of the different substrates.

After the  $\text{CdCl}_2$  treatment CdTe layers on glass/ITO/ZnO/CdS stacks lost the (111) preferred orientation and the peak (311) became predominant (see figure 7.4). In the case of CdTe deposited on polyimide/ITO/ZnO/CdS stacks the (111) preferential orientation is still strong, but (311) and (422) peaks have now similar intensity (see fig 7.4), so also in this case CdTe layers have more random orientation.

Solar cells produced on glass in our lab have performed efficiencies around 14 %. However when glass is substituted with polyimide, efficiencies go down to 10 %. Solar cells were separated from the glass before measuring the efficiency.

On figure 7.5 current-voltage characteristics of our best flexible and rigid cells are shown.  $V_{oc}$  and fill factor have similar values for cells made on glass and on polyimide attesting that a good p-n junction was formed in both cases. The small losses for the flexible case (less than 10% from the values of the rigid cell) are explained by imperfection in the fabrication process, namely by micro-cracks

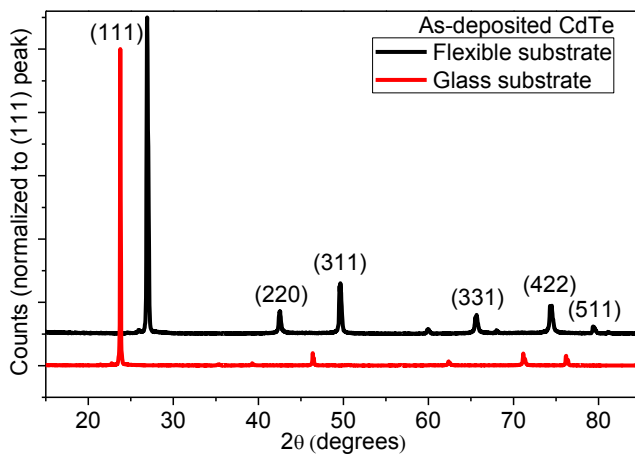


Figure 7.3: XRD patterns of the as-deposited CdTe on polyimide/ITO/ZnO/CdS (black) and glass/ITO/ZnO/CdS (red) stacks.

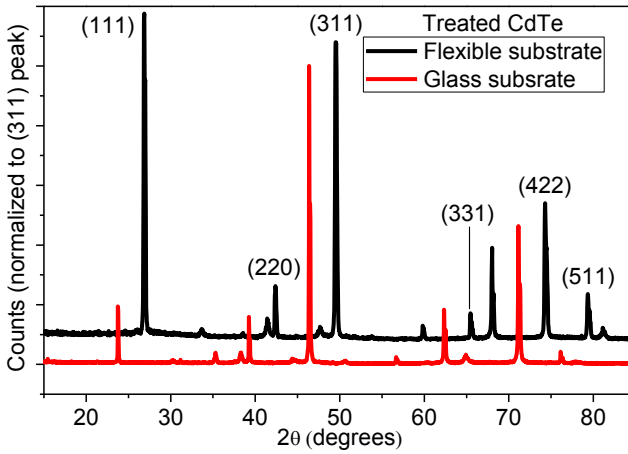


Figure 7.4: XRD patterns of the treated CdTe on polyimide/ITO/ZnO/CdS (black) and glass/ITO/ZnO/CdS (red) stacks.

of the films (due to the flexibility of the substrate) and by inhomogeneity of the wet treatment (because of the flatness problem).

However the main loss in flexible cells performance is due to the much lower current. This can be explained by the lower transparency of polyimide compared with glass [13]. In our case losses in current are in the range of 25 %, therefore more transparent substrates are required for higher efficiency.

### 7.4.2 Laser scribing

Single layers, namely TCO, CdS/CdTe and the back contact have been scribed with novel fiber lasers in order to test the feasibility of the industrial production of these devices. A new fibre laser made in the scope of the ALPINE project (Advanced Lasers for Photovoltaic INdustrial processing Enhancement) was used.

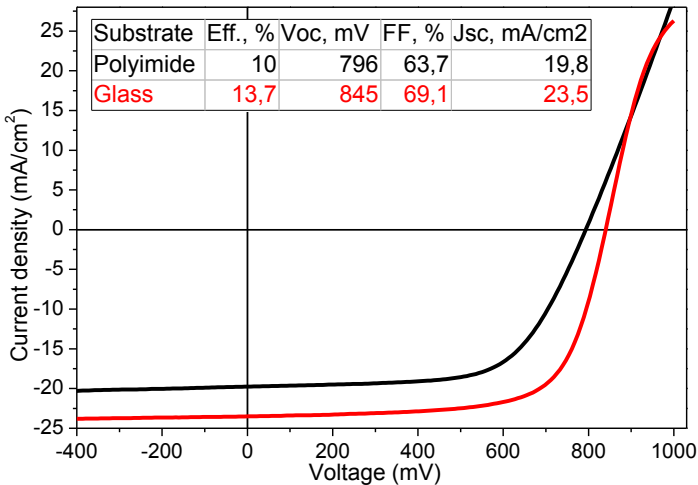


Figure 7.5: J-V curves of CdTe cells growth on polyimide (top) and on glass (bottom).

Fibre lasers offer a number of attractive features over traditional solid-state lasers. The emitted beam quality is independent of power and resistant to thermo-mechanical disturbances, thanks to single-

transverse mode wave guiding. These benefits, combined with high optical efficiency, compact and modular form factor, and support for alignment-free and monolithic packaging make pulsed-fiber sources destined for widespread use in scientific, medical and industrial applications. In particular, solar cell processing needs very precise and high throughput processes that can only be achieved with short pulses and/or short wavelengths.

The typical wavelengths for TCO of 1064 nm and for CdTe and back contact 532 nm have been used and pulses in the order of the hundred nanosecond range were applied.

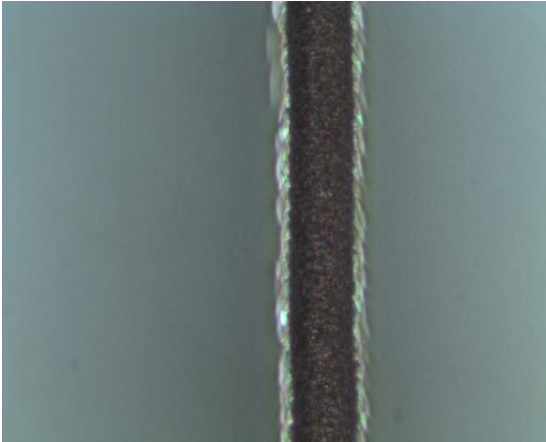


Figure 7.6: Laser scribe of polyimide/ITO/ZnO.

Laser scribing requires a flat surface in order to keep the scribes parallel to each other and to have the material under the laser focus, for this reason the flexibility of the solar cell is the main challenge. During the fabrication process polyimide was affected by high temperature, so that warping and some declension of flatness took place. Nevertheless P1 (removal of TCO) and P2 (removal of CdS/CdTe) scribing were applied to the stacks on flexible substrates showing very promising results.

For standard CdTe rigid solar cells, the ideal scribing process is with laser shining through the glass, so that vapors do not interfere with the beam. However attempts to scribe the TCO on polymer with this method tended to damage the polyimide. Better results were obtained by removing ITO/ZnO using film-side scribing (see figure 7.6).

P2 was provided by substrate-side scribing without damaging ITO and ZnO. To avoid any possible damage to the flexible substrate, tests were also made by scribing from the film side, however, CdTe ablation showed many imperfections, with some recasting in the middle of the scribe.

## 7.5 Conclusions

Solar cells with efficiencies exceeding 10 % were made; demonstrating the viability of flexible CdTe solar cells made with ITO front contact and wet CdCl<sub>2</sub> treatment.

The AFM analysis shows no significant difference in morphology of CdTe layers deposited on polyimide/ITO/ZnO/CdS stacks compared with CdTe on glass/ITO/ZnO/CdS.

The XRD measurements address the same recrystallization processes of the CdTe layers deposited on glass/ITO/ZnO/CdS and polyimide/ITO/ZnO/CdS stacks while as-deposited CdTe on polyimide/ITO/ZnO/CdS showed more randomized structure.

The efficiency drop for flexible cells is mainly due to the lower transparency of the polyimide substrate. Moreover wet treatment required further optimization in order to make this step more homogeneous.

Flexible cells on polymer substrates can be successfully scribed with a fibre laser, however a certain care has to be taken regarding the flatness to avoid damaging the polyimide. P1 and P2 steps were successfully applied to the stacks deposited on polyimide.

## 7.6 References

- [1] A. Salavei, I. Rimmaudo, F. Piccinelli, D. Menossi, N. Romeo, A. Bosio, R. Dharmadasa, A. Romeo, Proceedings of the 27th European Photovoltaic Solar Energy Conference, 2012.
- [2] First Solar Q3 Earnings Presentation, First Solar, November 1, 2012.
- [3] M.A. Green, Prog. Photovolt: Res. Appl. 19 (2011) 498–500.
- [4] A. Romeo, G. Khrypunov, F. Kurdesau M. Arnold, D.L.Bätzner, H. Zogg, A.N. Tiwari, Solar Energy Materials & Solar Cells 90 (2006) 3407–3415.
- [5] A.C. Vasko, X. Liu, A.D. Compaan, Photovoltaic Specialists Conference (PVSC), 34th IEEE (2009) 001552–001555.
- [6] J. Perrenoud, B. Schaffner, S. Buecheler, A.N. Tiwari, Solar Energy Materials & Solar Cells 95 (2011) S8–S12.
- [7] J. Drayton, A. Vasko, A. Gupta, A.D. Compaan, Conference Record of the 31st IEEE Photovoltaic Specialists Conference, (2005) 406–409.
- [8] Media release from EMPA, [http://www.empa.ch/plugin/template/empa/\\*/108277/---/l=2](http://www.empa.ch/plugin/template/empa/*/108277/---/l=2), June 9, 2011.
- [9] M. Chen, Z.L. Pei, C. Sun, J. Gong, R.F. Huang, L.S. Wen, Materials Science and Engineering B85 (2001) 212–217.
- [10] M.Girtan, Solar Energy Materials & Solar Cells 100 (2012) 153–161.
- [11] J. Pern, NREL/PR-520-44665, APP International PV Reliability Workshop, 2008.
- [12] A. Salavei, I. Rimmaudo, F. Piccinelli, V. Allodi, A. Bosio, N. Romeo, S. Mazzamuto, D. Menossi and A. Romeo, Proceedings 26th European Photovoltaic Solar Energy Conference, (2011) 3030–3034.

- [13] J. Perrenoud, S. Buecheler, A.N. Tiwari, Proceedings Photovoltaic Specialists Conference (PVSC), 34th IEEE, (2009) 000695–000699.



## 8 Final conclusions

A low temperature fabrication process for high efficiency CdS/CdTe solar cells in superstrate configuration was developed. It is based on the vacuum evaporation process and wet CdCl<sub>2</sub> treatment. CdS/CdTe solar cells with efficiencies exceeding 14.5 % are made with this process. The flexibility of the developed procedure was demonstrated: fabrication steps could be substituted with alternative ones without a significant drop in the solar cells efficiency.

Studying the effect of the Freon activation treatment on CdS/CdTe solar cells brings us to the conclusion that this activation process does not transform CdTe layers in the same way that CdCl<sub>2</sub> do. Solar cells activated with Freon treatment showed lower efficiencies comparing with solar cells activated by CdCl<sub>2</sub> treatment. Better results could be obtained by further understanding the influence of Freon treatment on CdS/CdTe stacks.

Study of the solar cells with thin CdTe absorbers brought us to the conclusion that high efficiency CdTe solar cells could be fabricated with a reduced CdTe thickness. Efficiencies exceeding 10 % were obtained for 1.5 μm thick absorbers.

When the CdTe thicknesses reduced lower than 1 μm, the CdS<sub>x</sub>Te<sub>1-x</sub> intermixed layer starts to affect the electrical performance of the solar cells, as it has become a significant part of the device.

It was shown that developed low substrate temperature fabrication process is suitable for fabrication of the solar cells on flexible substrates. The solar cells with efficiencies exceeding 10 % were made, demonstrating the viability of the flexible CdTe solar cells made with ITO front contact and wet CdCl<sub>2</sub> treatment.



## List of abbreviations

AFM	Atomic force microscopy
AM	Air mass
AR	Antireflective
Br-MeOH	Bromine in methanol
CBD	Chemical bath deposition
CIGS	Copper indium gallium di-selenide
DC	Direct current
$\eta$	Efficiency
FF	Fill Factor
FTO	Fluorine doped SnO <sub>2</sub>
GE	General Electric
J-V	Current density-voltage
I <sub>sc</sub>	Short circuit current
ITO	Indium tin oxide
MOCVD	Metal organic chemical vapour deposition
NREL	National Renewable Energy Laboratory
PVD	Physical vapour deposition
RF	Radio frequency
sccm	Standard cubic centimeters per minute
TCO	Transparent conductive oxide
VE	Vacuum evaporation
V <sub>oc</sub>	Open circuit voltage
XRD	X-ray diffraction
ZTO	Zinc stannate



## Acknowledgments

First of all I would like to thank Dr. Alessandro Romeo for the opportunity to work in his Group and for support, advice and supervision of my doctoral thesis.

I would further like to thank Ivan Rimmaudo with whom I had the pleasure to exchange ideas and to have discussions about CdS/CdTe solar cells and much more.

My thank goes to Valentina Allodi for the growth of CdS by CBD and for fruitful discussions.

I would like to thank Dr. Fabio Piccinelli for the XRD measurements.

I would like to thank Prof. Nicola Romeo and Dr. Alessio Bosio for possibility to use PVD technique from their laboratory.

My special thanks go to Dr. Daniele Menossi for fruitful discussions and for his patient help with growing TCOs for polymer samples.

Я хочу поблагодарить моих дорогих Папу и Маму за их веру в меня, терпение и поддержку. Спасибо Вам.

Спасибо тебе, Марина, за твою помощь и веру в меня.

Спасибо вам, мои дорогие Братья, без вас этого бы не случилось.

I would like to acknowledge the EU funded FP7 ALPINE Project, n. 229231, for supporting this work.



## List of publications

1. A. Salavei, I. Rimmaudo, F. Piccinelli, P. Zabierowski and A. Romeo Study of difluorochloromethane activation treatment on low substrate temperature deposited CdTe solar cells. *Solar Energy Materials & Solar Cells* 112 (2013) 190–195
2. A. Salavei, I. Rimmaudo, F. Piccinelli, A. Romeo Influence of CdTe thickness on structural and electrical properties of CdTe/CdS solar cells. *Thin solid films*, In Press, Corrected Proof, Available online 16 December 2012
3. I. Rimmaudo, A. Salavei, A. Romeo, Effects of activation treatment on the electrical properties of low temperature grown CdTe devices. *Thin solid films*, In Press, Corrected Proof, Available online 16 December 2012
4. A. Salavei, I. Rimmaudo, F. Piccinelli, D. Menossi, N. Romeo, A. Bosio, R. Dharmadasa, A. Romeo, Flexible CdTe Solar Cells by a Low Temperature Process on ITO/ZnO Coated Polymers. *Proceedings of the 27th European Photovoltaic Solar Energy Conference*, 2012
5. I. Rimmaudo, A. Salavei, A. Romeo, Ageing of CdTe Devices by Copper Diffusion. *Proceedings of the 27th European Photovoltaic Solar Energy Conference*, 2012
6. I. Rimmaudo, A. Salavei, F. Piccinelli, D. Menossi, N. Romeo, A. Romeo, Device and Physical Properties of Solar Cells with Thin CdTe Absorbers. *Proceedings of the 27th European Photovoltaic Solar Energy Conference*, 2012
7. A. Salavei, I. Rimmaudo, F. Piccinelli, V. Allodi, A. Romeo, A. Bosio, N. Romeo, S. Mazzamuto, D. Menossi, Low Substrate

Temperature Deposited CdTe Solar Cells with an Alternative Recrystallization Process Proceedings of the 26th European Photovoltaic Solar Energy Conference, 2011

8. V. Allodi, I. Rimmaudo, A. Salavei, A. Romeo, N. Armani, F. Fabbri, Study of Electro-Optical Properties of CdTe Solar Cells Prepared by a Low Temperature Fabrication Process, Proceedings of the 26th European Photovoltaic Solar Energy Conference, 2011
9. I. Rimmaudo, A. Salavei, V. Allodi, A. Romeo, P. Zabierowski, T. Drobiazg, A. Bosio, N. Romeo, S. Mazzamuto, D. Menossi, Electrical Characterization of CdTe Solar Cells Made by a Low Temperature Fabrication Process Proceedings of the 26th European Photovoltaic Solar Energy Conference, 2011
10. N. Romeo, A. Bosio, S. Mazzamuto, D. Menossi, J. L. Pena, A. Salavei, I. Rimmaudo, V. Allodi, A. Romeo, Investigation of a Suitable Back Contact for CdTe/CdS Solar Cells Prepared in the Substrate Configuration, Proceedings of the 26th European Photovoltaic Solar Energy Conference, 2011

## Curriculum vitae

Name: Andrei L. Salavei  
Date of birth: 3rd of July, 1981  
Place of birth: Minsk, Belarus

### Education

Present  
2013 Postdoctoral research fellow, Laboratory for Applied Physics, University of Verona

2012  
2010 PhD student, Laboratory for Applied Physics, PhD Program in Nanotechnologies and Nanostructured Materials for Biomedical Applications, University of Verona

2005  
2003 Master of Science (technical sciences), Electronic Technique and Technology Department, Belarusian State University of Informatics and Radioelectronics, *thesis*: “Investigation of discharge characteristics under ion beam assisted magnetron deposition”

2003  
1998 Electronics Engineer, Faculty of Computer-Aided Design, Belarusian State University of Informatics and Radioelectronics, Certificate of degree-high distinction diploma, *thesis*: “The integrated ion-plasma system”